DETECTION AND VISUALISATION OF CLIMATE TRENDS IN CHINA

by

GEMMER, Marco*; BECKER, Stefan*; JIANG, Tong**

No. 15, Giessen, November 2003

* Department of Geography, Justus-Liebig-University,
Senckenbergstrasse 1, 35390 Giessen, Germany

** Nanjing Institute of Geography and Limnology,
Chinese Academy of Science (CAS), 210008 Nanjing, PR China

CONTENTS

LIST OF FIGURES

PREFACE AND ACKNOWLEDGEMENTS

Research on climate trends in China has been carried out within a co-operation of the Justus Liebig Universities Department of Geography and Zentrum für internationale Entwicklungs- und Umweltforschung (ZEU) and the Nanjing Institute of Geography and Limnology (CAS). First results were introduced by BECKER et al. 2003 a, b who worked on precipitation trend analyses in the Yangtze River Catchment. In the meanwhile, the National Climatic Centre of China (NCCC) kindly provided climatic data in China within the framework of this co-operation. Financial support from the CAS Key project KZCX3-SW-331 and the NSFC project 40271112 enabled the data acquisition. The analysis of both, precipitation and temperature data for the whole of China from 1951-2002 can be carried out now.

A shorter version of the precipitation trend observation will soon be published in Theoretical and Applied Climatology (GEMMER et al. 2003, accepted for publication/in print). Results of the temperature trend research have not been published yet. They will be submitted to an international Journal when further statistical approaches with regard to daily temperature data are processed.

The discussion paper in hand will make the actual results accessible for further research groups in Germany.

1 INTRODUCTION

Causes and regional impacts of climatic change or variability have been widely discussed under various aspects. The means for detecting climate trends and variability are time-series analyses based on data sets e.g. of air temperature, air pressure, precipitation, humidity, and cloudiness. The latest IPCC report (IPCC 2001) indicates a 30–50% increase of precipitation in southern China in the winter months (December, January, February) from 1900-1999. An inconsistent pattern with an increase in the western and a decrease in the eastern Yangtze catchment is detected in the summer months (June, July, August). ZHAI et al. (1999a) show a significant increase in precipitation over the middle and lower reaches of the Yangtze River and west China during the latter part of the 20th century, while also detecting a declining trend in precipitation over northern China (from IPCC 2001). The report also describes an increase of the surface temperature in east China between 0.5 and 2°C and up to

3°C in northern China from 1949-1997. The increase of temperature in northern China adds up to 1°C per decade from 1976 to 2000. This is mainly due to strong increases in the absolute minimum temperatures since the 1950s and an increase of hot days in the same period of time. This process can be described by the decreasing number and intensity of cold waves (ZHAI et al. 1999b).

The distribution and seasonal variations of precipitation and temperature in China have been described by QIAN & ZHU (2001); QIAN et al. (2002); DOMRÖS & PENG (1988), and DOMRÖS (2001). The implications of climatic variations regarding air temperature and precipitation are particularly relevant for China as to its regional disparities of natural resources. Climatic variations can increase the occurrence of droughts and floods due to the unequal availability of water. These implications are a severe concern for China's agriculture and food security especially in the arid regions of northern China (see SMIT & CAI 1996). Higher temperatures will enhance the demand for water, particularly for human consumption and agriculture. Highly vulnerable regions will face increased risks of summer water shortages. Increasing temperatures will also alter water quality significantly by influencing water temperatures, discharges, runoff rates and timing, and the ability to assimilate pollutants.

The most recent example is the higher number of floods in the Yangtze river catchment in the 1990s and the water shortage in the Yellow river catchment which both have been aggravated by human activities and impacts of climatic change (GEMMER & KING 2003; KING et al. 2001). With regard to these tendencies, the detailed analysis of precipitation and temperature variations are important for the assessment of climate induced risks and countermeasures. Monthly trends of precipitation and temperature in China from 1951-2002 will therefore be analysed in the current study. Geographic techniques will be used for a spatial visualisation of climate trends.

2 DATA AND METHODOLOGY

The data set of 160 National Meteorological Observatory (NMO) stations with long-term monthly precipitation and temperature data in China have been analysed in this study. They have been provided by the National Climatic Centre (NCCC) of the China Meteorological Administration (CMA) and contain values from January 1951 to December 2002. The location of the stations can be seen in **figure 1**. The density of stations is lower in the sparsely populated high mountainous and desert area of west and north-west China.

The homogeneity of the precipitation and temperature records was analysed by calculating the von Neumann ratio (N), the cumulative deviations ($Q/n^{-0.5}$ and $R/n^{-0.5}$), and the Bayesian procedures (U and A) (BUISHAND 1982; MANIAK 1997). The data sets of all stations which have been used in the present study are homogeneous with a significance beyond the 95% confidence level.

The trends of monthly precipitation and temperature sums have been analysed by applying the Mann-Kendall trend test for all of the 160 stations. Confidence levels of 90%, 95%, and 99% were taken as thresholds to classify the significance of positive and negative precipitation trends. Trends at a significance below the 90% confidence level were not considered.

Figure 1: Location of the stations (both precipitation and temperature) in China

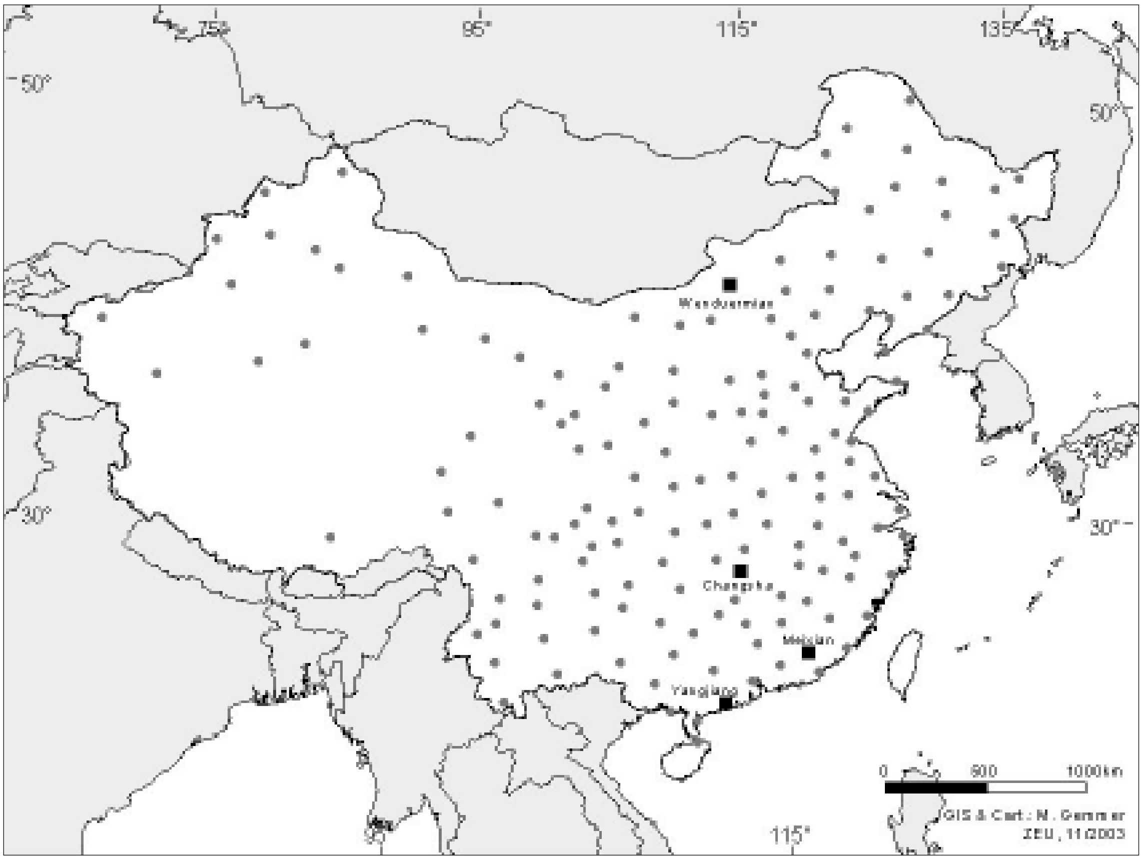

The observed trends were spatially interpolated by applying the Inverse Distance Weighted (IDW) interpolation method. IDW creates a raster surface. The raster cell values are calculated by averaging the values of station data in the vicinity of each cell. Station data in this paper refer to the confidence levels of trends at the 160 stations. IDW implies that each station has a local influence that decreases with distance (DE BY 2001). The interpolated raster surface is based on a weighted average of the station values. The value of each cell is mostly influenced by nearby points and less by more distant points. The IDW method requires the specification of the power parameter and the search radius. The power parameter controls the significance of calculated station values upon the interpolated values. By defining a high power, more emphasis is placed on the nearest points, and the resulting surface will have more detail. The power parameter in the IDW interpolation was set to 6.

The choice of the relatively high power ensures a high degree of local influence and giving the output surface increased detail. The search radius has been specified by choosing a number of 4 neighbouring stations, i.e. the spatial interpolation has been carried out within a fixed radius of 4 neighbouring stations (see BILL 1999). It is not meaningful to analyse the regional structure of precipitation and temperature trends for the whole of China by applying and comparing different interpolation methods. Applying other interpolation methods (e.g. kriging) result in similar output maps. This is due to the available number of stations and the scale of the projection and the magnitude of the research area, respectively. The interpretation of the results of different interpolation methods would only be feasible for smaller areas or a higher station density.

3 PRECIPITATION

3.1 Observed Precipitation Trends

Both, positive and negative precipitation trends at all confidence levels exist in each month (**figure 2**). January, July, September, and November are the months which show the highest number of trends in both positive and negative direction. The smallest number of trends can be observed for March, October, and December. Also SCHÄFER (2001) points out inconsistent annual precipitation trend patterns in the Yangtze river catchment with positive trends in some parts of the middle and lower catchment since 1951. Many positive trends can be noted in January, June, and July. Negative trends prevail in February, September and November. A relatively equal number of stations with both positive and negative trends can be detected in August, October and December.

Figure 2: Observed Precipitation Trends at the 90, 95, and 99% Confidence Level

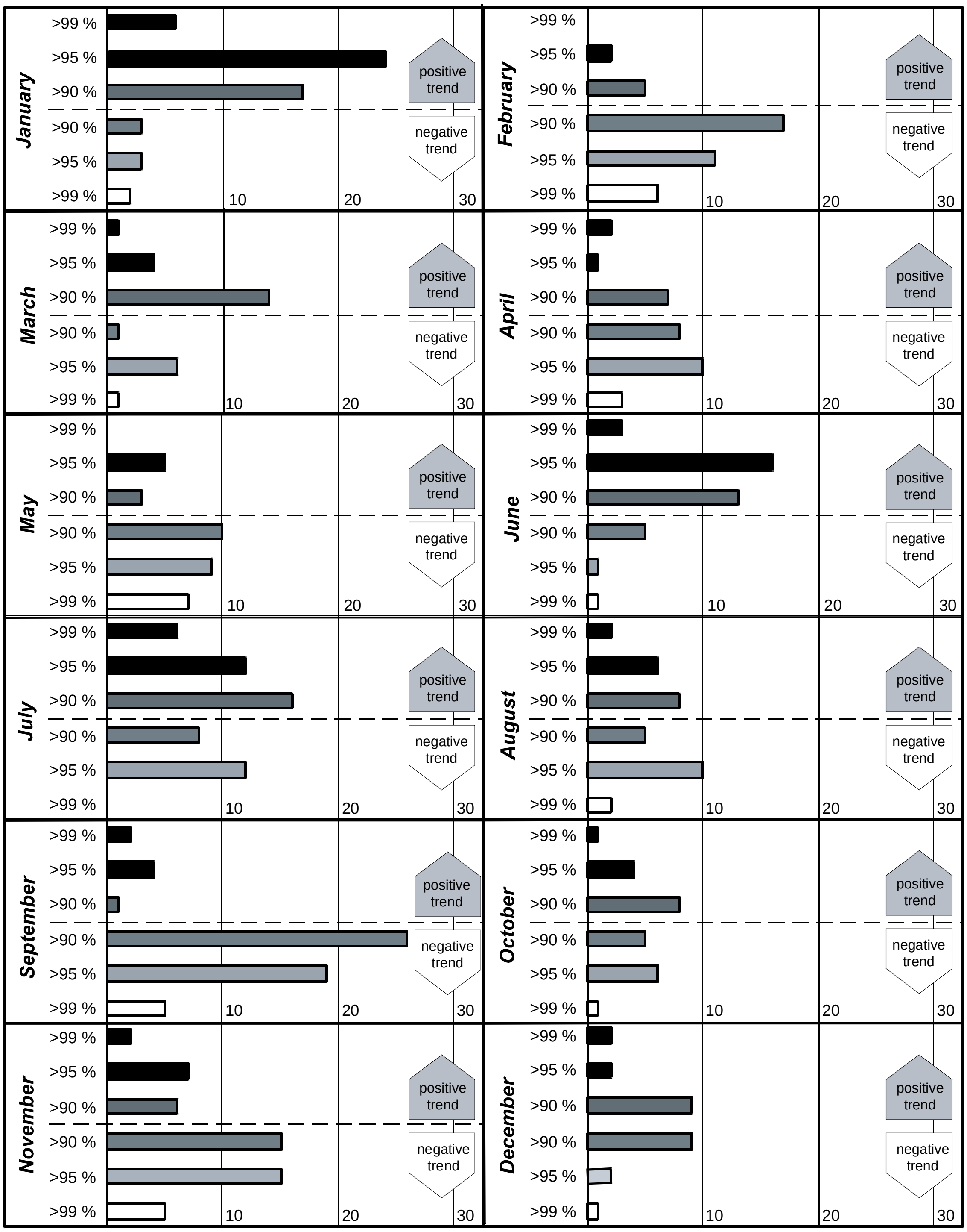

Figure 3 displays examples of significant positive and negative precipitation trends at four stations in January and July to illustrate the order of magnitude of the investigated trends (see **figure 1**). The graphs show the monthly precipitation sums 1951-2002 (thin grey line) and the attached linear trends (thick black line). The R^2 values show that a maximum of 18% of the variation can be explained by the linear regression. The

increase of precipitation over the last 51 years reaches values beyond 150% of the base level. This illustrates the order of magnitude of the investigated trends. The location of the stations is highlighted in **figure 1**.

3.2 Interpolated Precipitation Trends

Figures 4-15 show the interpolated monthly precipitation trends in China during 1951-2002. The projection of the map illustration is Lambert Equal-Area Azimuthal (central meridian 108°). The displayed classes are based on the confidence levels which are discussed in chapter 2. As can be seen, the spatial illustration of the detected precipitation trends enables a better understanding of climatic changes or variations in China within the last 50 years, especially regarding the uneven spatial distribution of precipitation trends.

Figure 4 reveals that the relatively high number of positive trends in January mainly refers to stations which are located in a belt which covers the middle and lower Yangtze river catchment as well as Dongting and Poyang lake catchments (see **figure 16**). These stations are mainly situated in the lowlands and the foothills of the adjoining mountain ranges. Another agglomeration of positive precipitation trends is located in the highlands of Sichuan and Qinghai provinces (see **figure 17**). Moreover, some isolated stations with positive and negative precipitation trends can be found in the very west and north-east of China.

The relatively high number of negative precipitation trends in February (**figure 5**) results mainly from stations in the north-east and the Xinjiang, Gansu, and Inner Mongolia provinces/autonomous regions. Isolated positive precipitation trends occur in the high mountainous regions of Tibet, Qinghai, and Xinjiang provinces (see **figure 17**). The belt of positive precipitation trends in March (**figure 6**) stretches along the southern and eastern high mountainous region of the Qinghai-Tibet-Plateau. Further positive trends can also be detected in the eastern coastal region of China whereas negative trends occur in the north-east (catchment of the Hailar river), north-north-east (inner flow catchment of Inner Mongolia) and north-west (western Tarim basin, catchment of Manas and Aibi lakes) (see **figure 16**).

Figure 3: Examples of Significant Positive and Negative Precipitation Trends at Four Stations in January and July

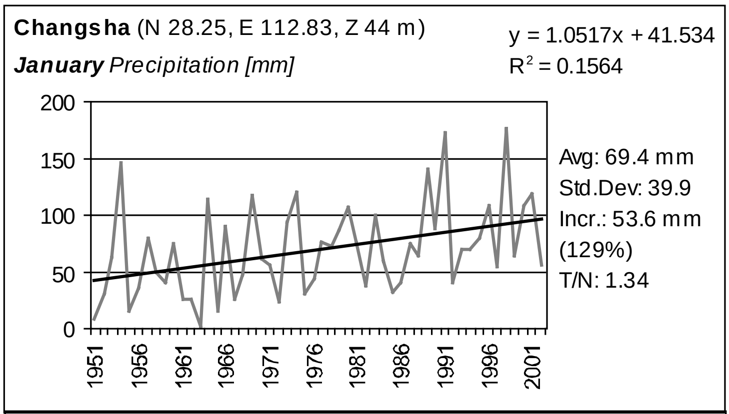
Changsha (N 28.25, E 112.83, Z 44 m)
January Precipitation [mm]
y = 1.0517x + 41.534
R2 = 0.1564
Avg: 69.4 mm
Std.Dev: 39.9
Incr.: 53.6 mm
(129%)
T/N: 1.34

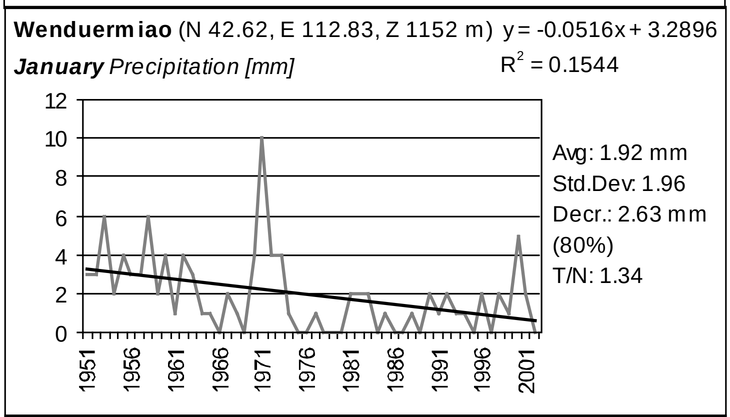
Wenduermiao (N 42.62, E 112.83, Z 1152 m)
January Precipitation [mm]
y = -0.0516x + 3.2896
R2 = 0.1544
Avg: 1.92 mm
Std.Dev: 1.96
Decr.: 2.63 mm
(80%)
T/N: 1.34

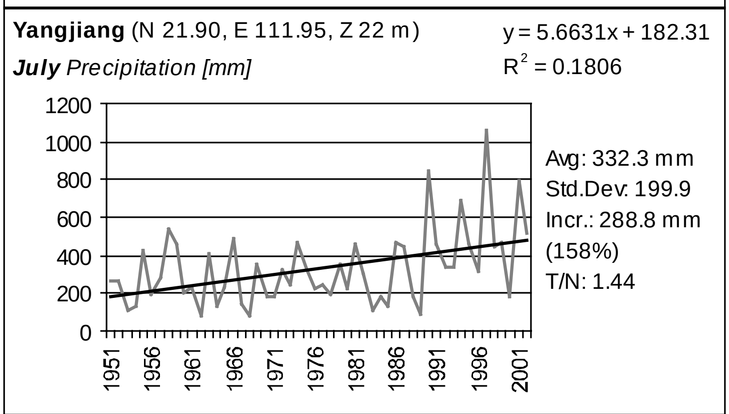
Yangjiang (N 21.90, E 111.95, Z 22 m)
July Precipitation [mm]
y = 5.6631x + 182.31
R2 = 0.1806
Avg: 332.3 mm
Std.Dev: 199.9
Incr.: 288.8 mm
(158%)
T/N: 1.44

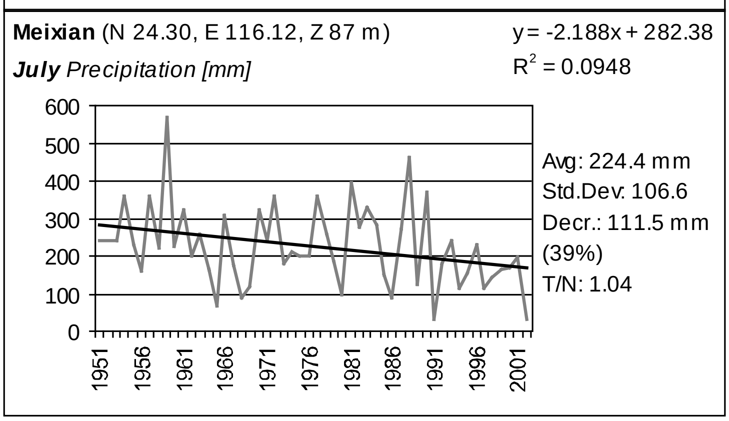
Meixian (N 24.30, E 116.12, Z 87 m)
July Precipitation [mm]
y = -2.188x + 282.38
R2 = 0.0948
Avg: 224.4 mm
Std.Dev: 106.6
Decr.: 111.5 mm
(39%)
T/N: 1.04

Figure 4: Mann-Kendall Precipitation Trend Test January 1951-2002

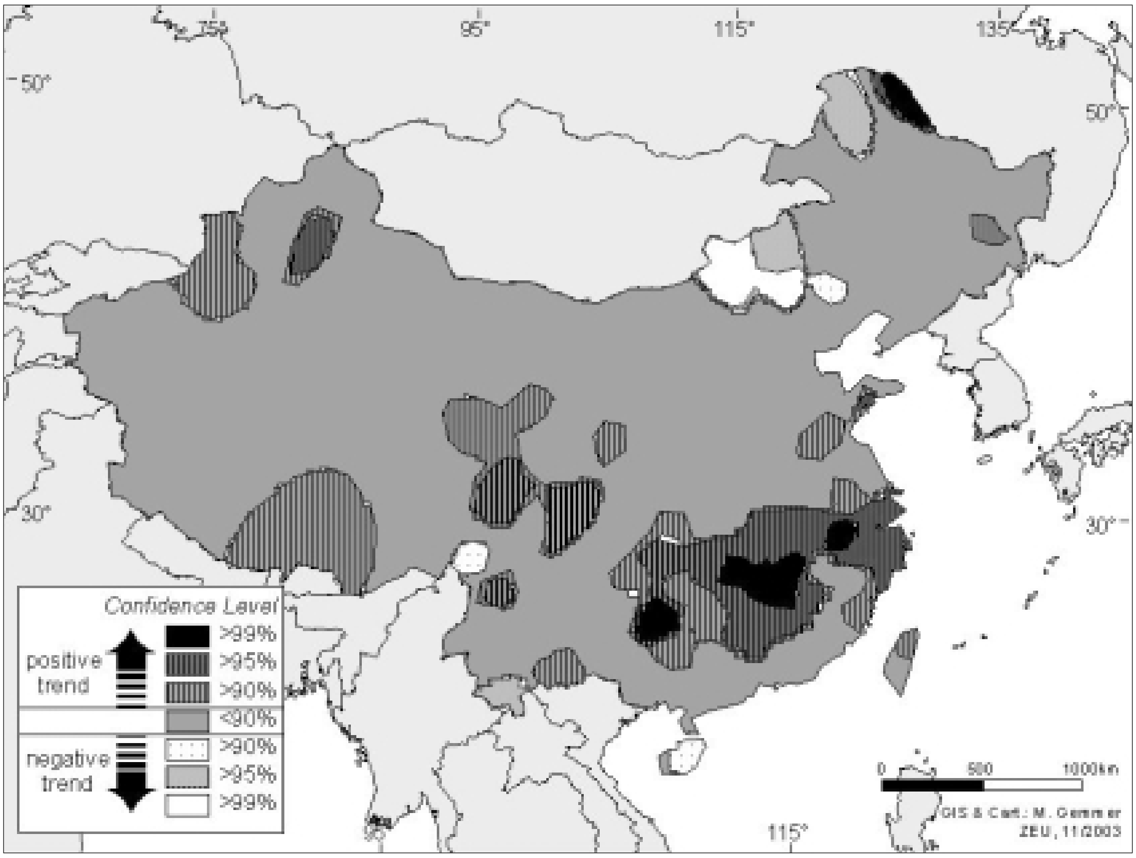

Figure 5: Mann-Kendall Precipitation Trend Test February 1951-2002

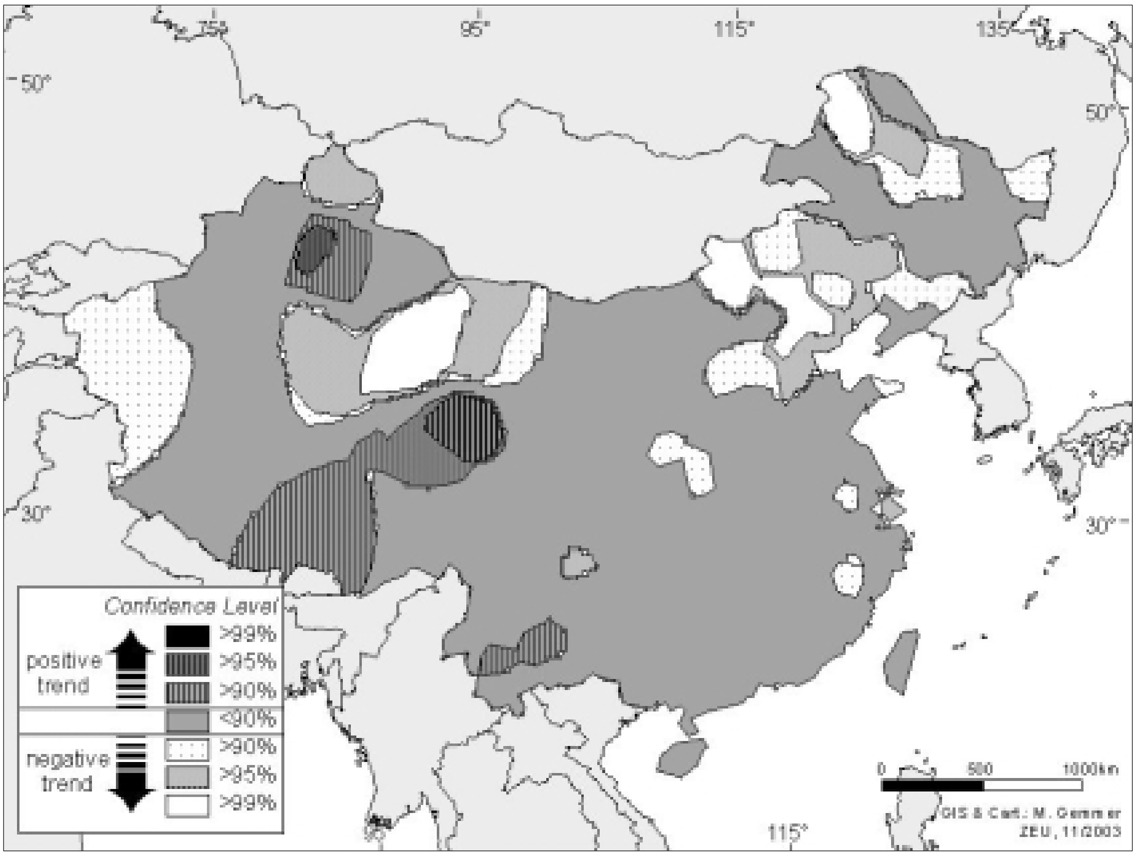

Figure 6: Mann-Kendall Precipitation Trend Test March 1951-2002

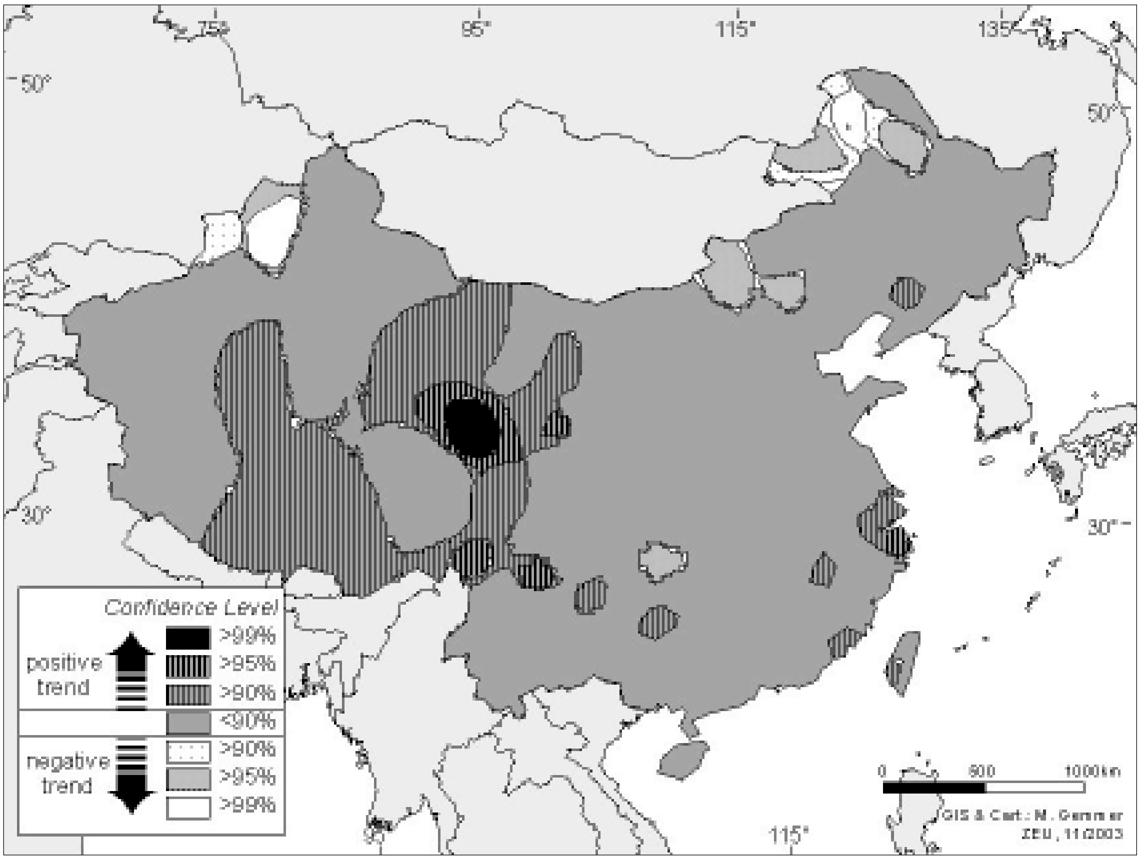

Different precipitation trend patterns can be recognised in April (**figure 7**). The stations in the high mountainous regions of southern Qinghai and north-eastern Tibet province that were excluded from the positive trend belt in March show positive precipitation trends in April. No significant trend can be detected for the surrounding stations. Isolated stations with negative and positive trends are spread widely over central and eastern China. An uninterrupted belt of stations with negative trends is located in the catchment areas of the Lower Yangtze, Huaihe, Hanjiang, and Huanghe (see **figure 16**).

Figure 8 depicts precipitation trends in May which are dominated by an extended region of negative trends in the Middle and Lower Yangtze river catchment, particularly the catchments of Dongting, Poyang and Tai Lakes, as well as the south-eastern coastal catchment. Further stations with negative trends stretch along the mountain ranges which mark the western Sichuan basin. Insular stations with positive trends can be found mainly in western China.

Figure 7: Mann-Kendall Precipitation Trend Test April 1951-2002

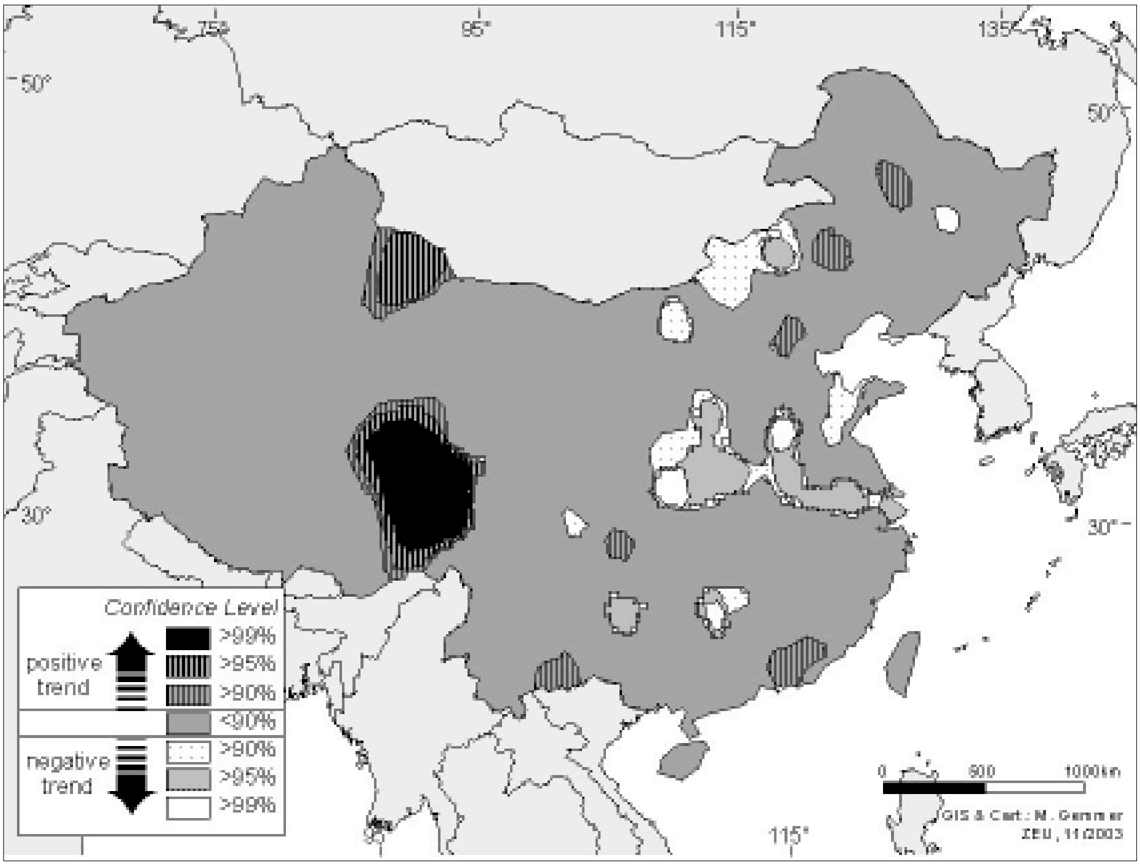

A dominating feature of June trend map (**figure 9**) is the extended region with positive trends that stretches from north to south in central China only to be interrupted by the Min and Qin mountain ranges north of Sichuan province. Insular stations with mainly positive trends are spread over the rest of China.

Precipitation trend patterns in July (**figure 10**) follow the three topographical features of China. Whereas large parts of the south-east Lowlands and the western mountainous regions are dominated by positive trends we observe negative trends along the transition zone of the middle ranged mountain axis from central to north-east China.

Figure 8: Mann-Kendall Precipitation Trend Test May 1951-2002

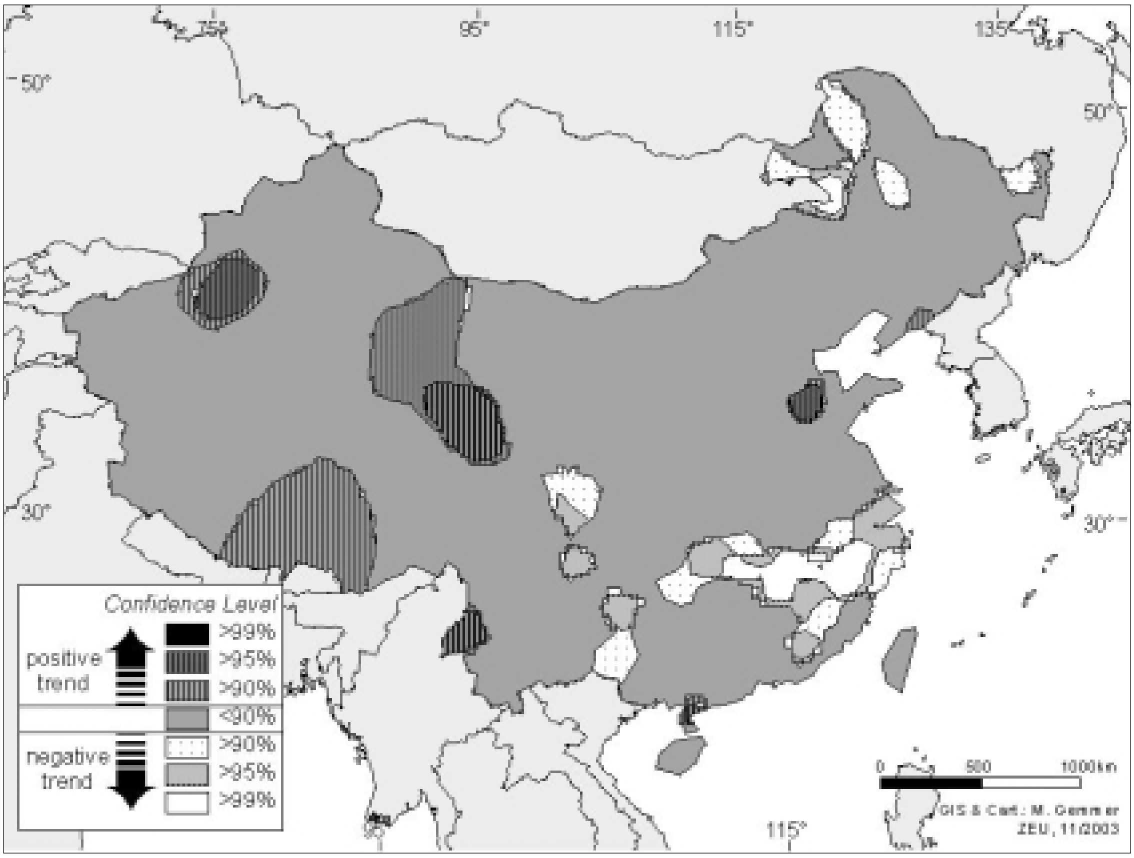

Figure 9: Mann-Kendall Precipitation Trend Test June 1951-2002

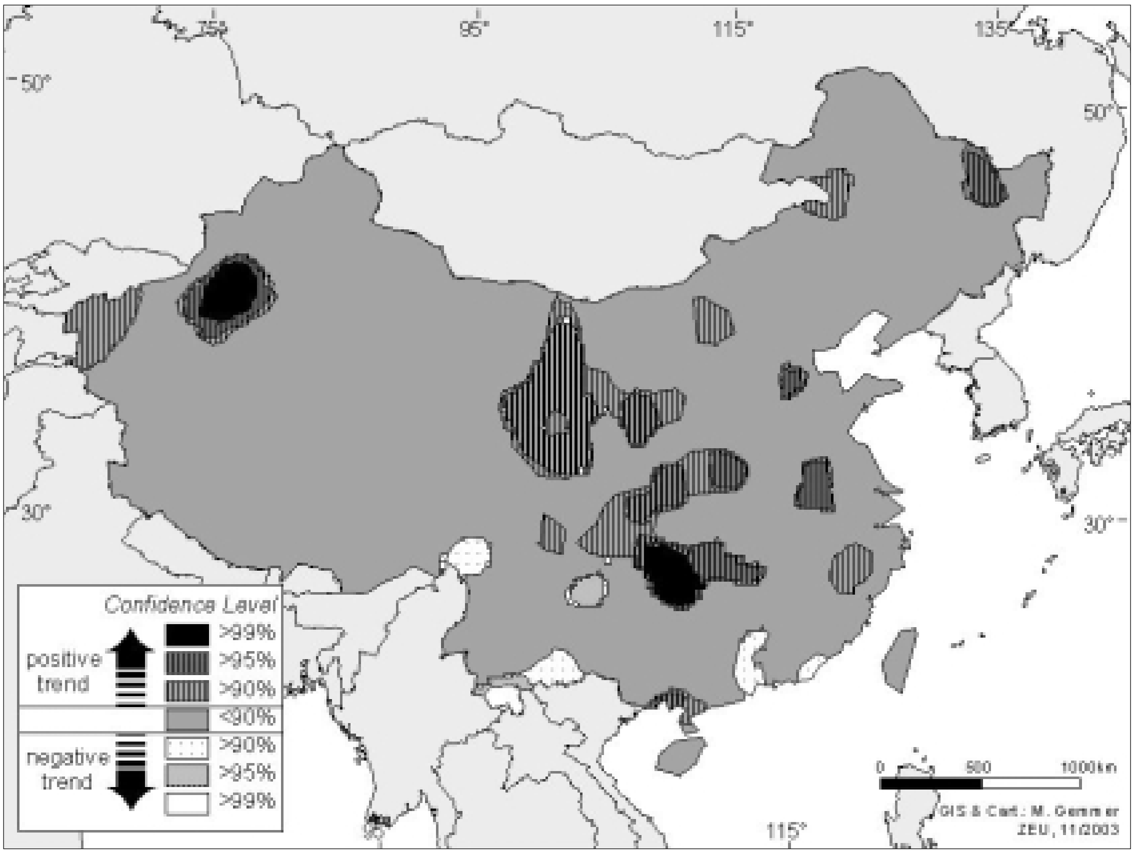

Figure 10: Mann-Kendall Precipitation Trend Test July 1951-2002

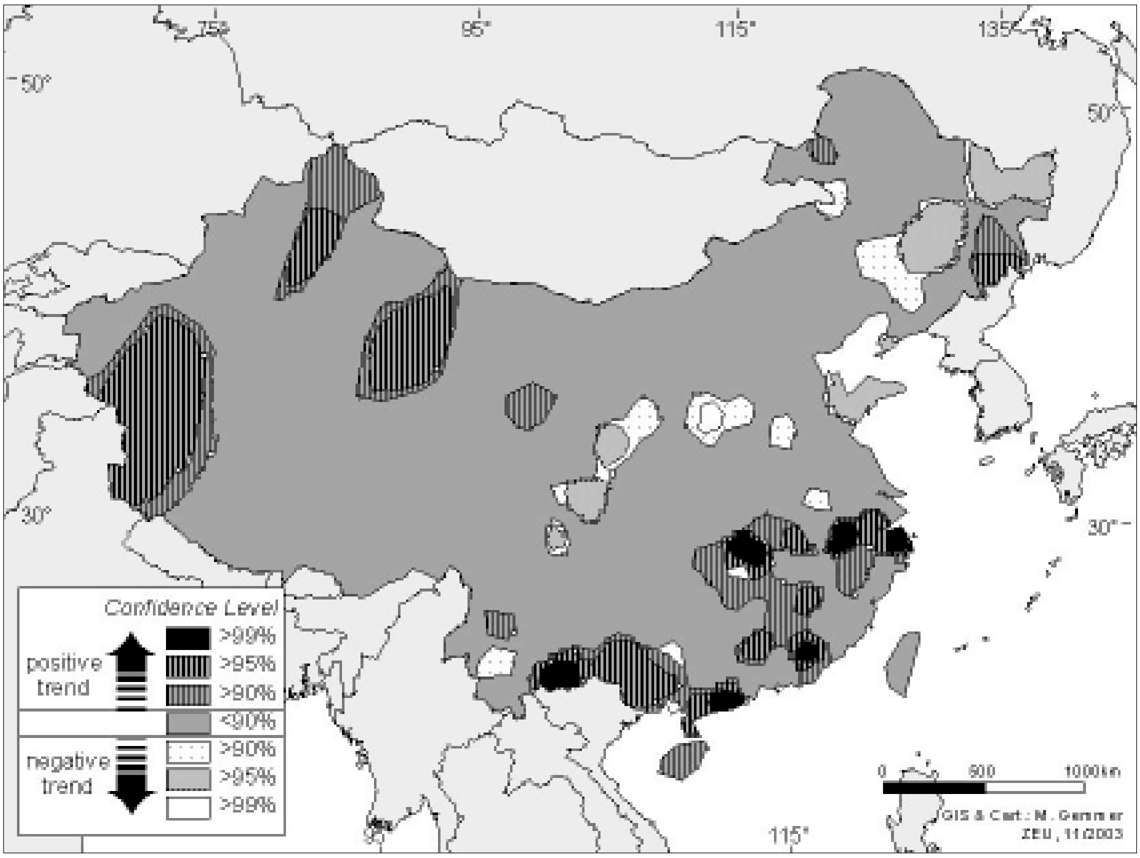

Positive trends in August (**figure 11**) are mainly confined to the south-east and east coastal regions. Negative trends are concentrated in the Huaihe catchment in north-east China and spread insularly over the rest of the country. **Figure 12** depicts a concentration of negative precipitation trends in September. They can mainly be found in Gansu and Sichuan Province (central China), the lower Yangtze and the eastern coastal regions, and the north-east up to the Dahinggan mountains. Positive trends are concentrated in southern Tibet and western Yunnan provinces (see **figure 17**).

Only a few number of stations without any recognisable underlying spatial agglomeration display positive and negative precipitation trends in October (**figure 13**). The number of stations with positive and negative trends is nearly equal as can also be seen in **figure 2**.

Figure 11: Mann-Kendall Precipitation Trend Test August 1951-2002

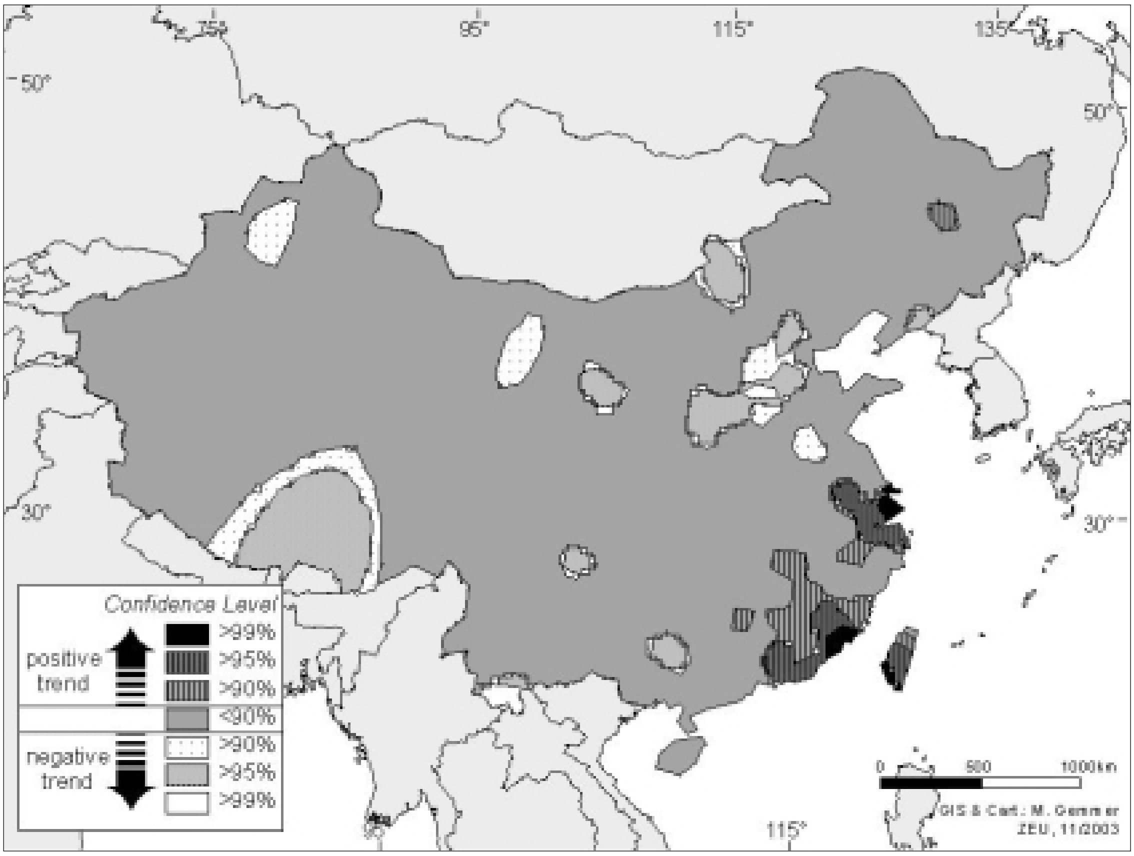

Figure 12: Mann-Kendall Precipitation Trend Test September 1951-2002

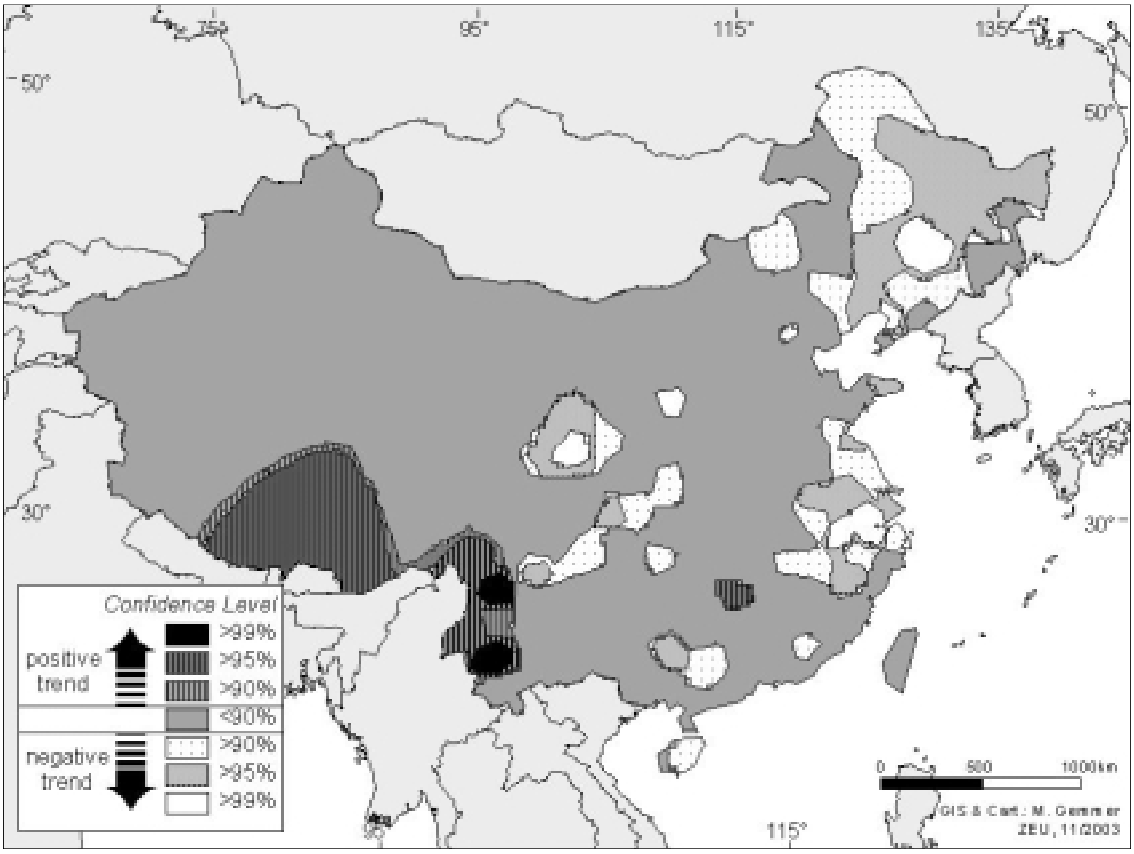

The November precipitation trend map (**figure 14**) is dominated by negative trends which cover large parts of the Huanghe, Huaihe, Haihe, Hanjiang, and Jialing catchments in central and eastern China as well as large parts of Tibet and Xinjiang provinces in west China. Positive trends dominate in the Yunnan plateau and stretch into Sichuan, Tibet, and Qinghai provinces (see **figures 16 and 17**).

Figure 13: Mann-Kendall Precipitation Trend Test October 1951-2002

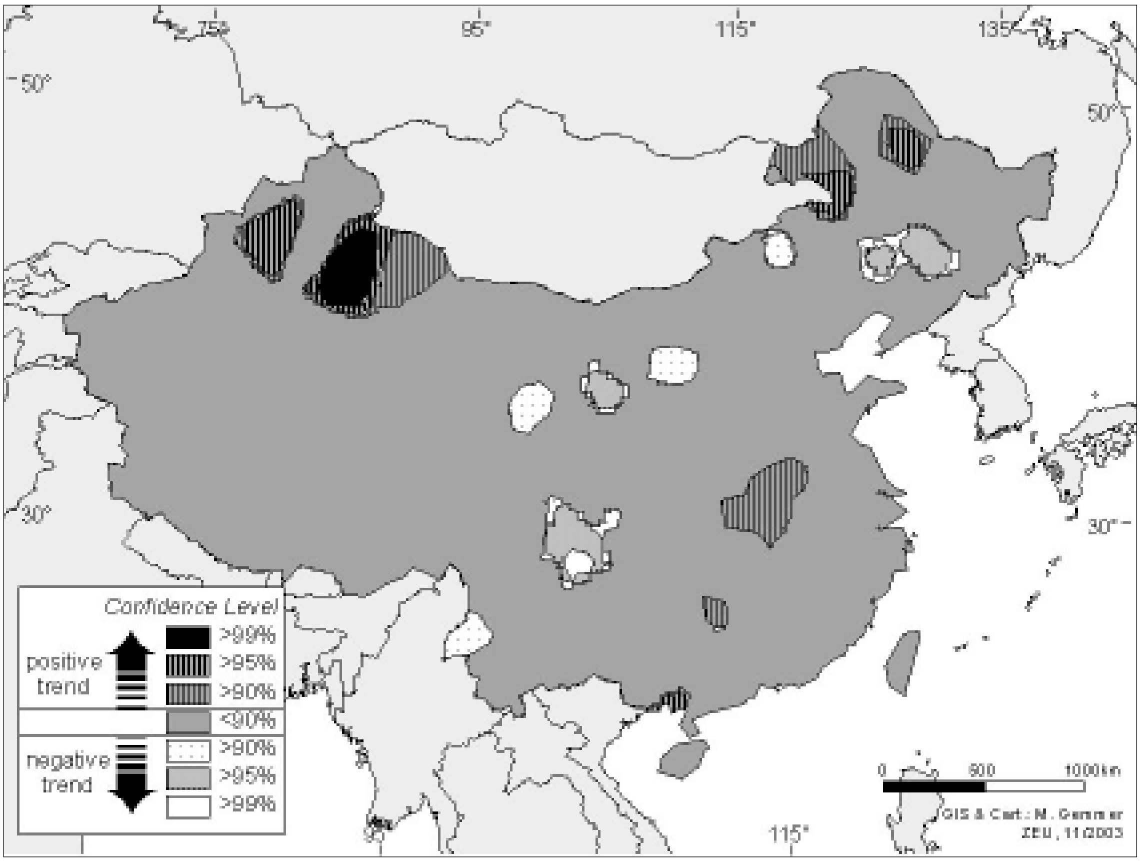

Comparatively few stations without any recognisable underlying spatial agglomeration display positive and negative precipitation trends in December (**figure 15**). The number of stations with positive and negative trends is nearly equal as can also be seen in **figure 2**.

Figure 14: Mann-Kendall Precipitation Trend Test November 1951-2002

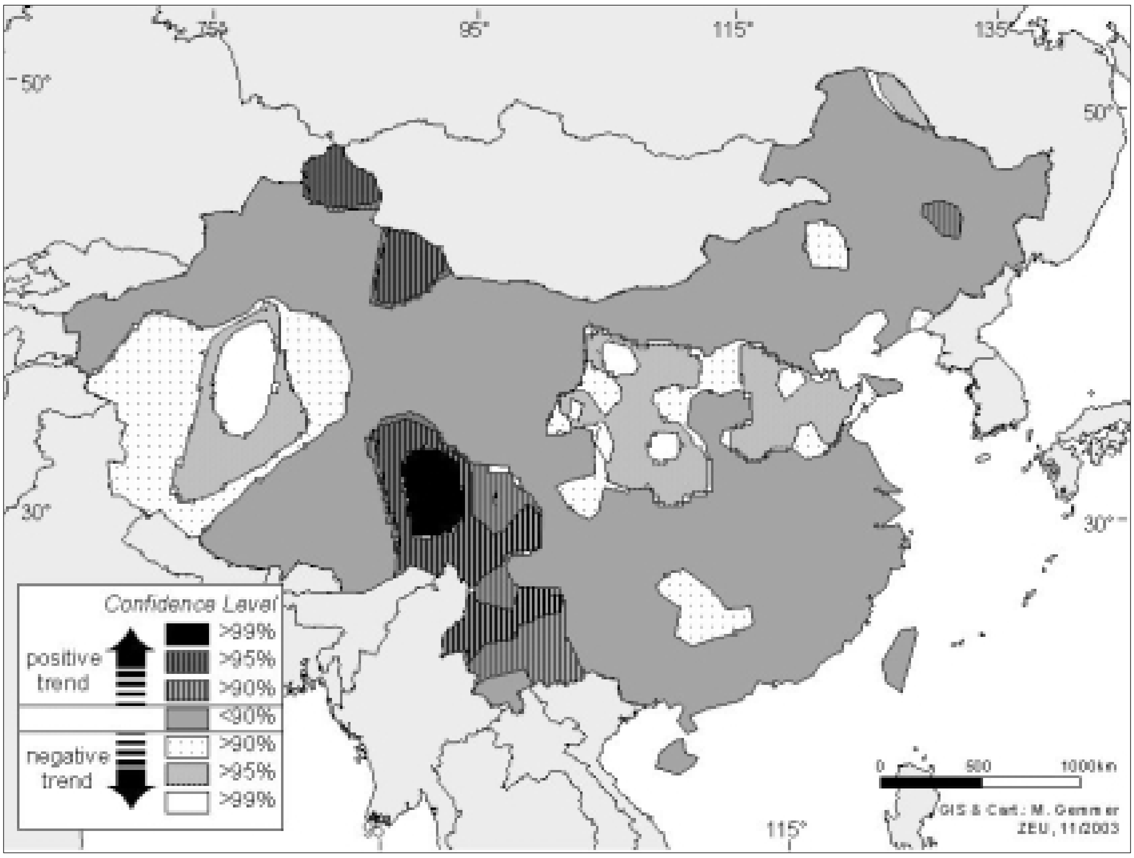

Figure 15: Mann-Kendall Precipitation Trend Test December 1951-2002

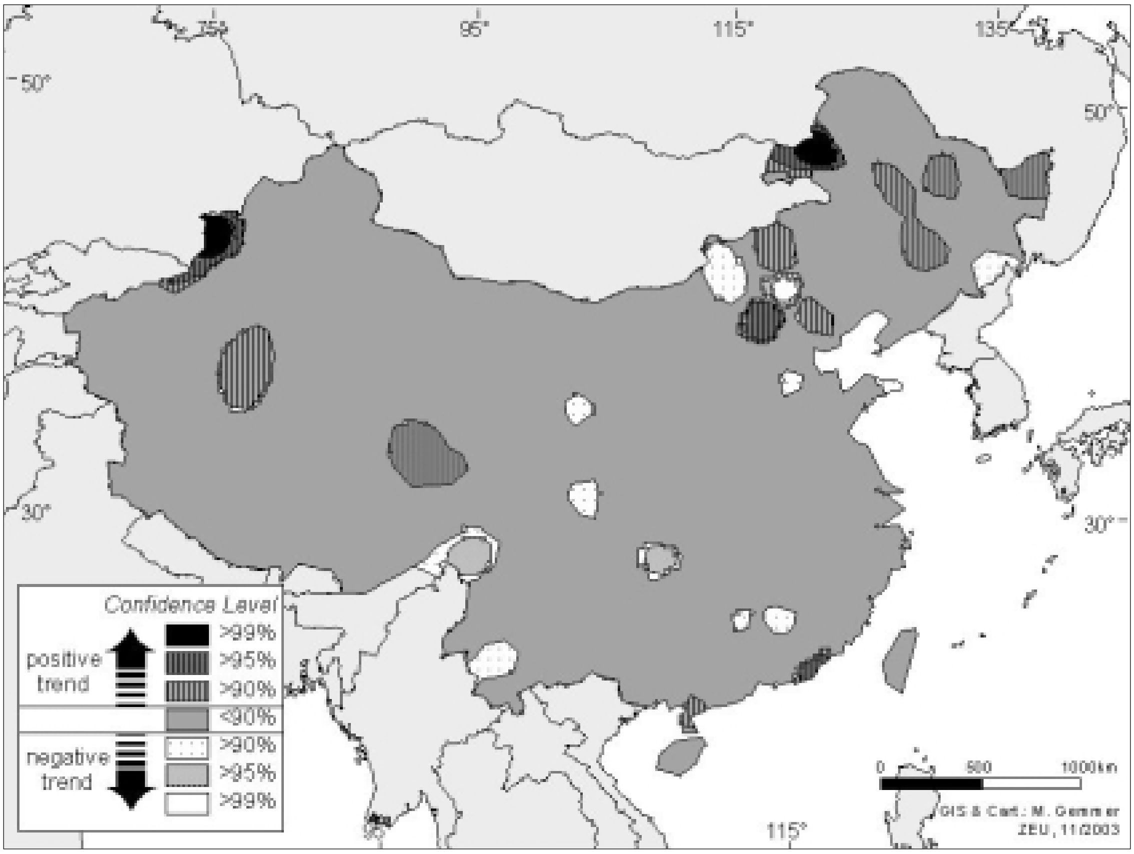

Figure 16: Big River Catchments in the PR China

Figure 17: Provinces, Autonomous Regions, and Municipalities of the PR China

4 TEMPERATURE

4.1 Observed Temperature Trends

One of the most apparent features of the temperature analysis is a distinct trend towards higher air-temperatures. It is true that both, positive and negative trends can be detected for the temperature time-series in China from 1951-2002 (**figure 18**). However, in contrast to the precipitation trends, positive and negative temperature trends are unbalanced. Positive trends predominate the Mann-Kendall trend test results. In January, February, and April more than 100 of the 160 stations underlie trends which are mostly positive. The highest number of negative trends can be assigned to July and August. The smallest number of trends in both directions can be noted for August and November.

It is noteworthy that positive trends at the 90, 95 and 99% confidence level are apparent in every month. Only a limited number of stations show negative trends, which can hardly be detected at all confidence levels during one month. In January and February for example, only one station shows negative temperature trends at a time.

These findings underline results from earlier studies which describe a general winter warming in the mid-high latitudes due to a weaker cold wave activity starting in the late 1970s/early 1980s (ZHAI et al. 1999b). Furthermore, the upward trend tendency are consistent with those of YIN 1999 and QIAN & ZHU 2001.

Generally speaking, the warming in China did not only occur during winter time but also during all other seasons. The results also support the IPCC report (2001), which states that the temperature has been submitted to an increase in the Northern Hemisphere during the 20th century.

Figure 18: Observed Temperature Trends at the 90, 95, and 99% Confidence Level

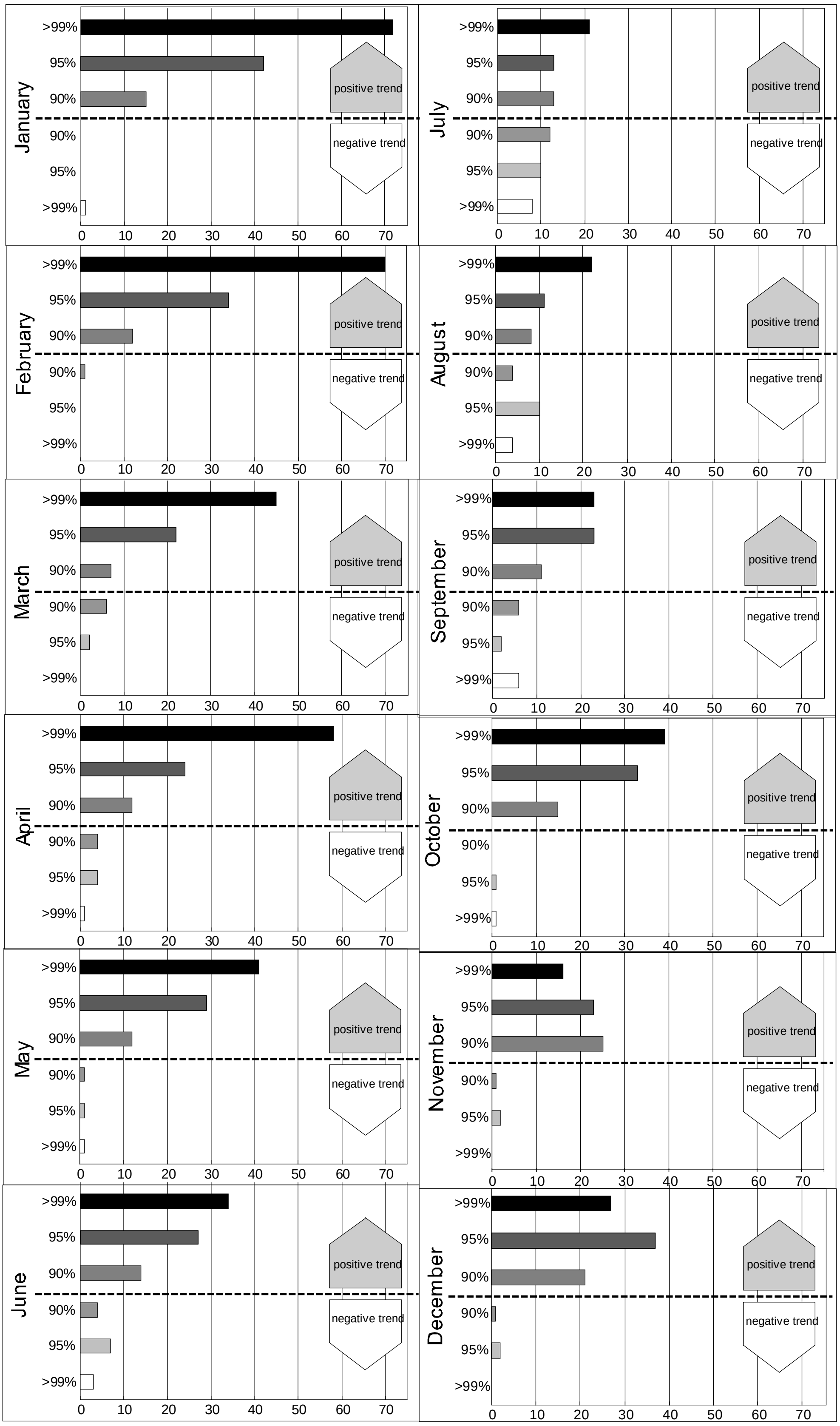

4.2 Interpolated Temperature Trends

Figures 19-30 show the interpolated monthly temperature trends for China from 1951-2002. The displayed classes are based on the confidence levels which are discussed in chapter 2. As can be seen, the spatial illustration of the detected temperature trends enables a better understanding of climatic changes or variations in China within the last 50 years, especially regarding the uneven spatial distribution of the trends. In addition, the unbalance of positive and negative temperature trends are better visible through the geographic visualisation.

Figure 19 reveals that the relatively high number of positive trends in January mainly refer to stations which are concentrated in two belts which cover the western mountainous area (Tibet) as well as the arid regions of north-west (Xinjiang), north (Inner Mongolia), and north-east (Beijing region) China (see **figure 17**). The agglomeration of positive stretches a long distance south and covers the eastern parts of the Yangtze, Huaihe and Huanghe catchments (see **figure 16**). Moreover, some isolated stations with positive and negative precipitation trends can be found in the north-east and south-west of China. The temperature increase in January can mainly be assigned to the northern and western part of the country.

Figure 19: Mann-Kendall Temperature Trend Test January 1951-2002

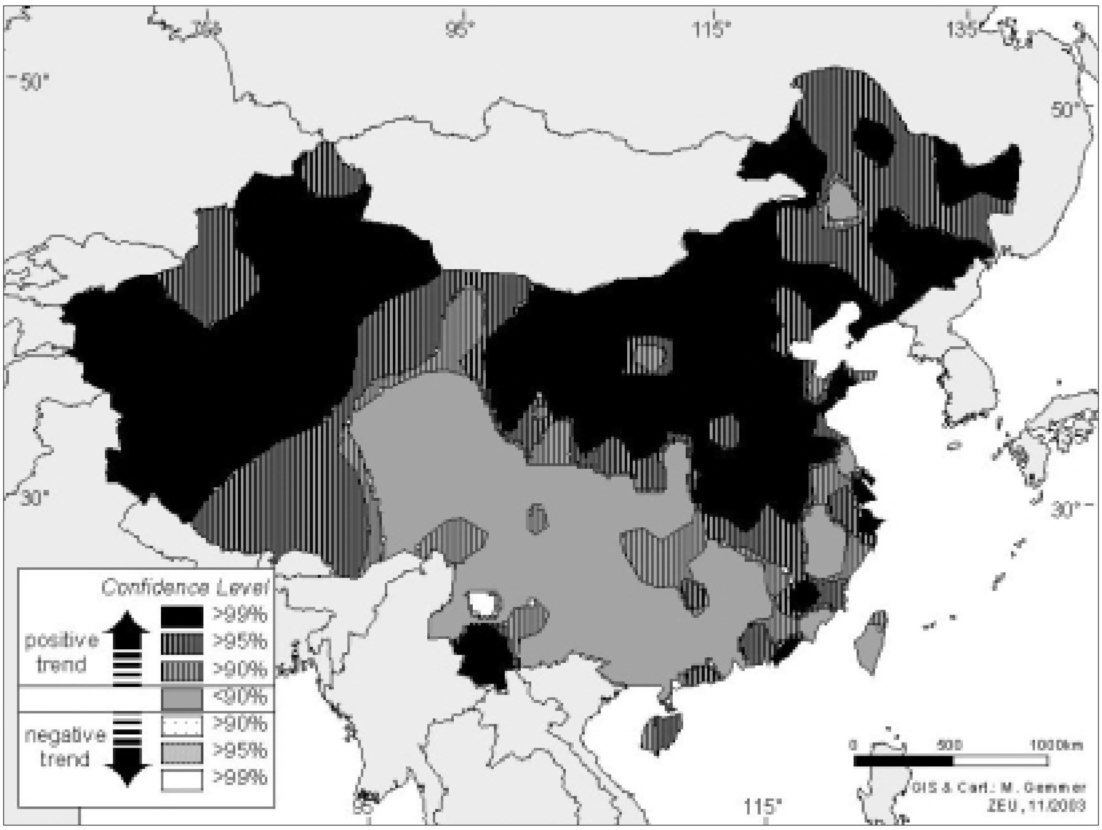

The relatively high number of positive temperature trends in February (**figure 20**) result from stations all over China except the southern coastal region and central China. The total north-east and parts of Xinjiang province are covered by positive trends beyond the 99% confidence level. Positive trends above the 90 and 95% confidence level can be assigned to the entire western part of the country and the middle and lower catchments of the Yangtze, Huaihe, and Huanghe rivers. The only station with negative trends in February is located in south-west China. It is the only station which has negative trends in January, too.

Figure 20: Mann-Kendall Temperature Trend Test February 1951-2002

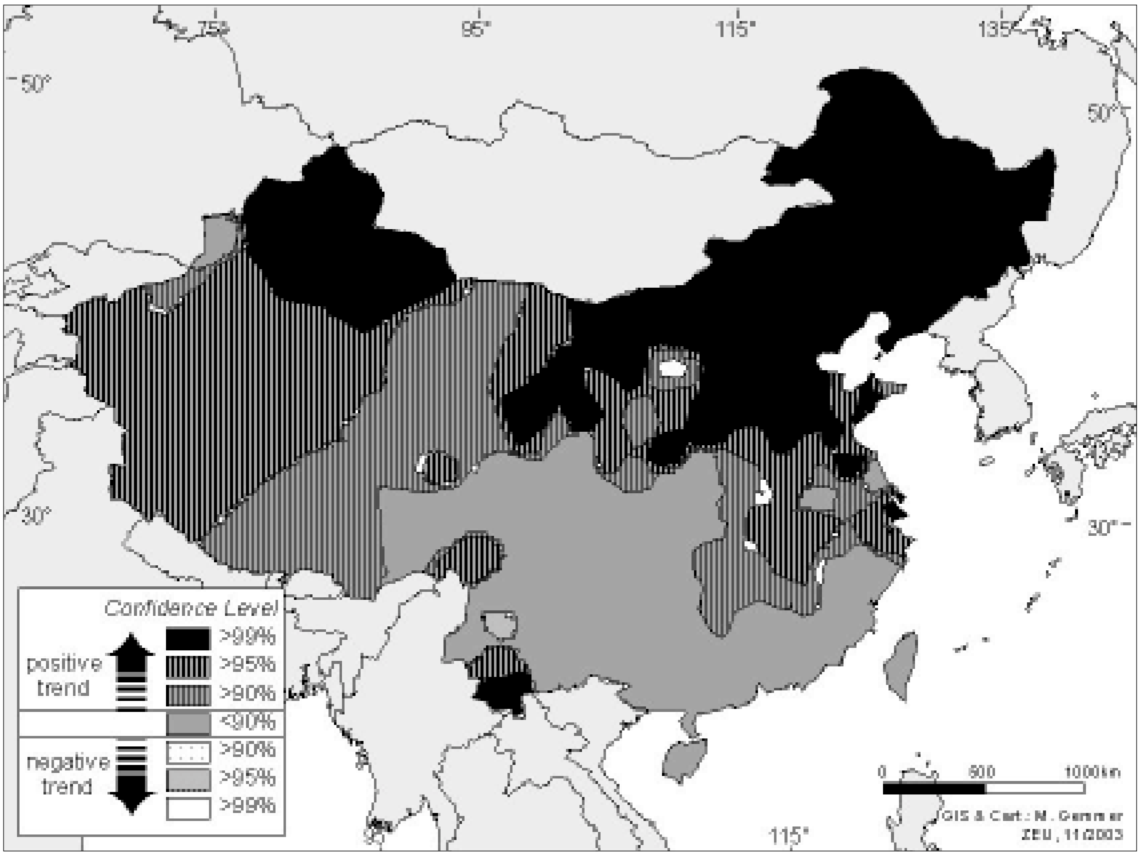

The spatial distribution of the temperature trends in January and February are very similar. Except of a few stations in central China, differences can only be noticed for the confidence levels of the positive temperature trends. Positive temperature trends in March (**figure 21**) are concentrated in north-east China and central Tibet (see **figure 17**). This agglomeration of significant positive trends corresponds to the findings of the previous months and is also valid for the southern part of Yunnan province. However, negative trends cover large parts of central China and the arid region at the Tarim inner flow area (Xinjiang province) in north-west China.

Figure 21: Mann-Kendall Temperature Trend Test March 1951-2002

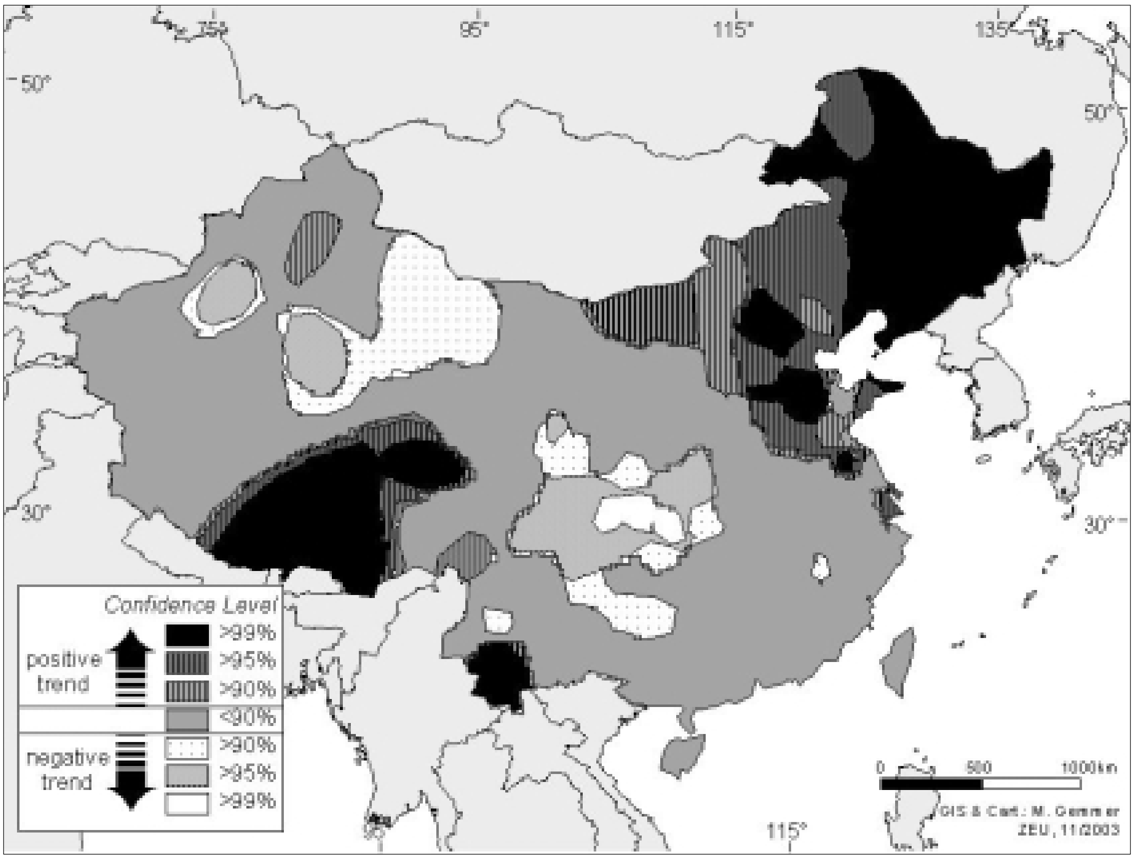

Figure 22: Mann-Kendall Temperature Trend Test April 1951-2002

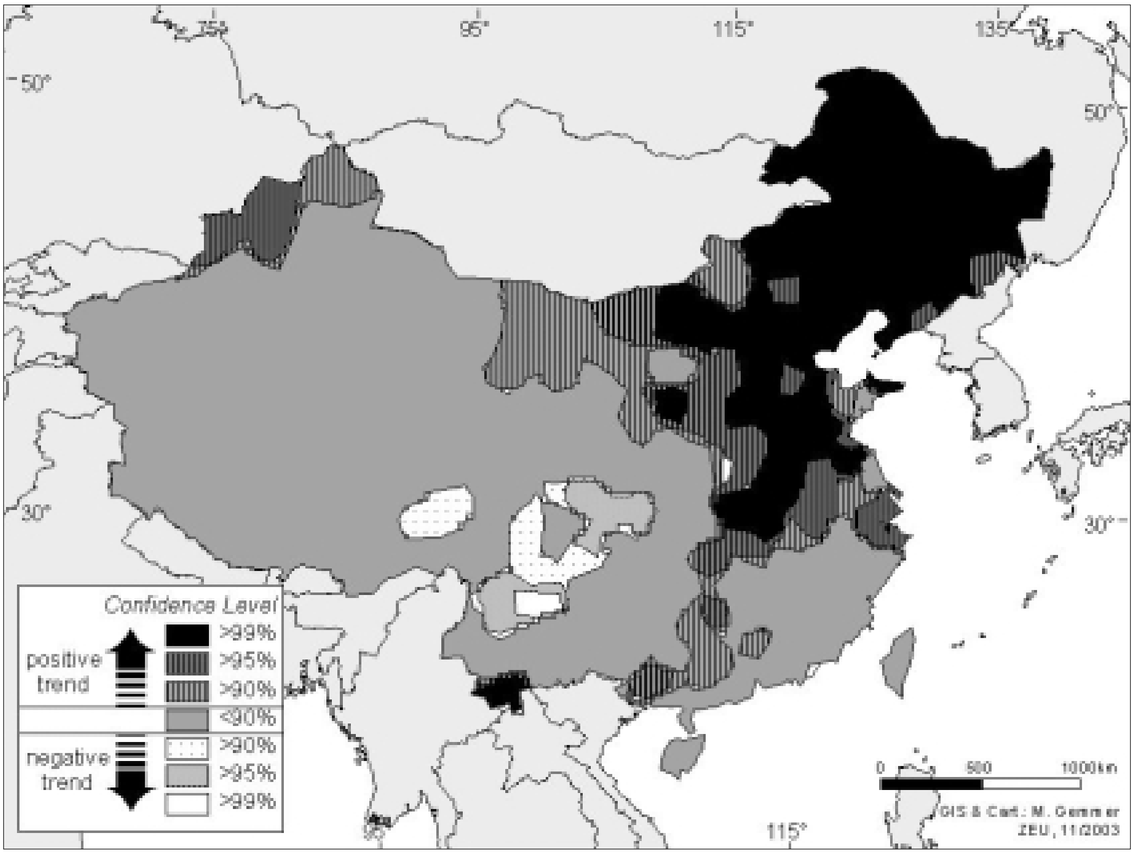

Temperature trend patterns in April (**figure 22**) do not differ greatly from the situation in March except the number of the stations with underlying trends. Stations in central China are distinguished by negative trends whereas positive trends prevail in north-east China. Nevertheless, no trend can be recognised in Tibet and western China in April except of the north-western part of Xinjiang province. An uninterrupted belt of stations with positive trends is located in the catchment areas of the middle Yangtze, Huaihe, Hanjiang, and Huanghe rivers and stretches right to Zhujiang river in the very south of China (see **figure 16**). This belt of trends lines out the topographical steps from the eastern lowlands to the central Chinese highlands.

Many isolated trends patterns can be recognised in May (**figure 23**). The figure depicts an extended belt of positive temperature trends in the middle and lower Yangtze catchment and in Inner Mongolia. Isolated stations with positive trends line up along a latitudinal line right from the Beijing region over to Qinghai, Tibet and Xinjiang. Negative trends are restricted to a smaller area in Xinjiang and some isolated stations which stand alone in southern China.

Figure 23: Mann-Kendall Temperature Trend Test May 1951-2002

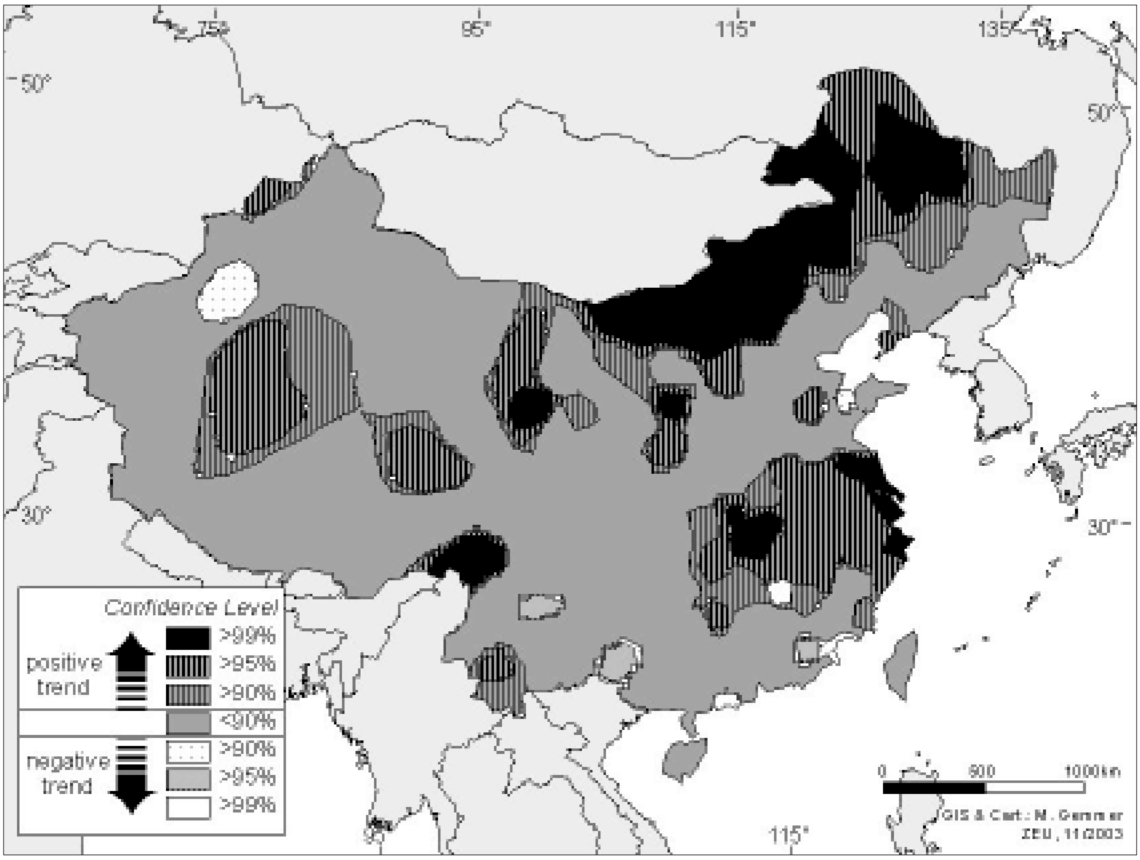

The number and spatial extent of negative temperature trends is increasing in June (see **figure 24**). Again they can be found in central China where they form a consistent pattern. Further negative trends cover large parts of Xinjiang and a smaller area in Gansu province/Inner Mongolia. Positive trends prevail in central Tibet, Yunnan, the southern coastal region and the entire Hainan island. The only interruption of the trend belt is along the Vietnam boundary. A second agglomeration of positive trends can be detected in north-east China. It covers the eastern part of Inner Mongolia and great parts of the Helongjiang catchment.

Figure 24: Mann-Kendall Temperature Trend Test June 1951-2002

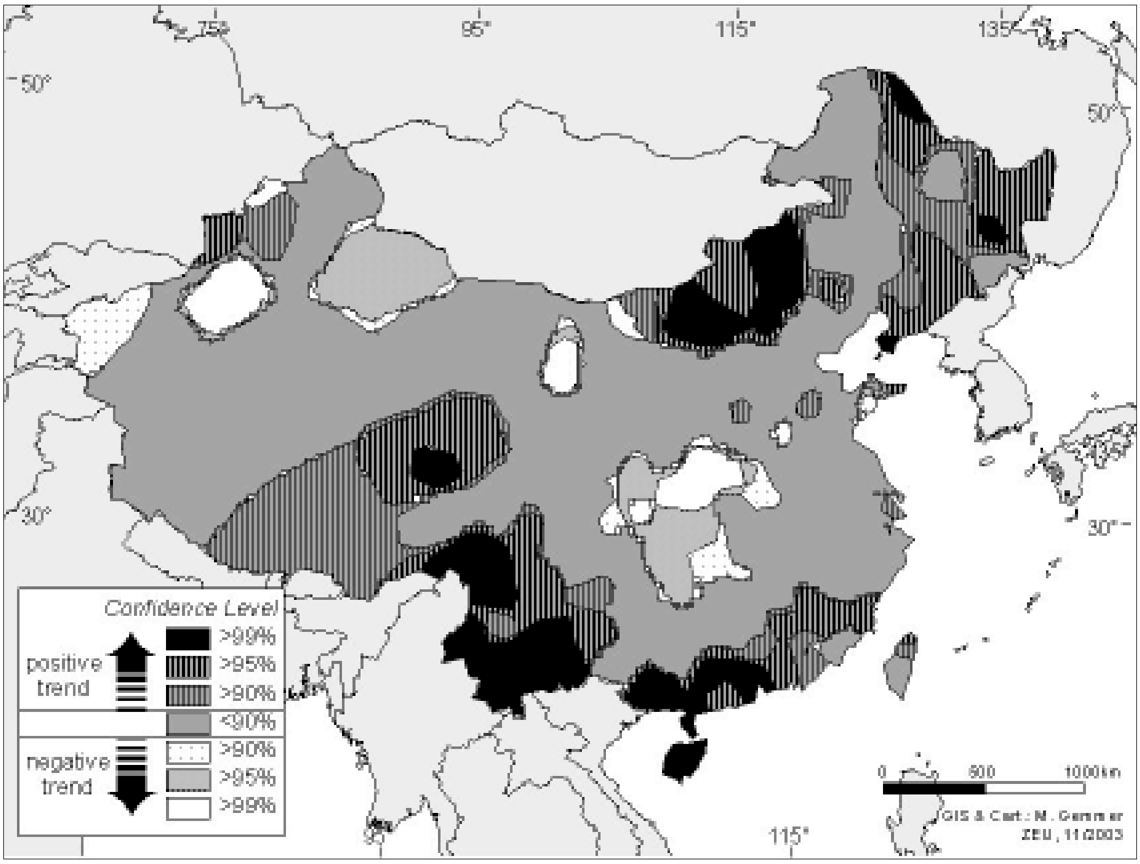

The highest number of negative temperature trends can be detected in July (**figure 25**). Central and south-central China is dominated by negative trends. They also occupy exactly those areas in Xinjiang and Inner Mongolia which have experienced negative trends in March and June. They are also confined to the outer border regions in the north-east (Helongjiang), north (Inner Mongolia), north-west (Xinjiang), south-west (Tibet and Yunnan), and southern coastal region. Hainan island is distinguished by positive trends as well. The absolute number of negative trends is lower than the one of positive trends. The map highlights negative trends due to their spatial concentration.

Figure 25: Mann-Kendall Temperature Trend Test July 1951-2002

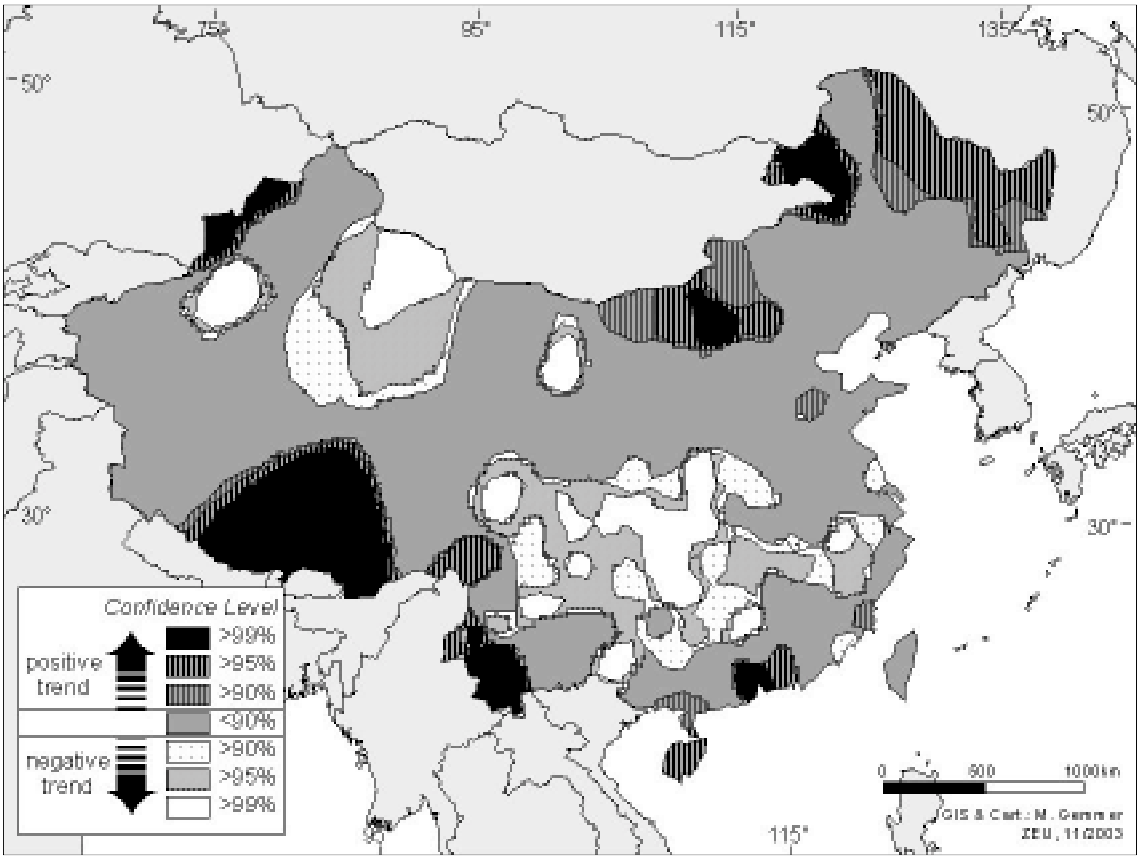

Positive temperature trends in August (**figure 26**) are mainly confined to the south-west and the southern coastal region, but the trend belt shows a considerable spatial extension from Xinjiang and Tibet to Guangdong (see **figure 16**). Figure 26 also depicts a concentration of positive trends in Inner Mongolia. Negative trends are concentrated in the arid region of Xinjiang, Qinghai and Gansu covering large areas. They insularly cover the lowlands of south-east China and the southern Yangtze catchment and spread over the rest of the country. August is the month with one of the highest detected numbers of negative temperature trends.

Figure 26: Mann-Kendall Temperature Trend Test August 1951-2002

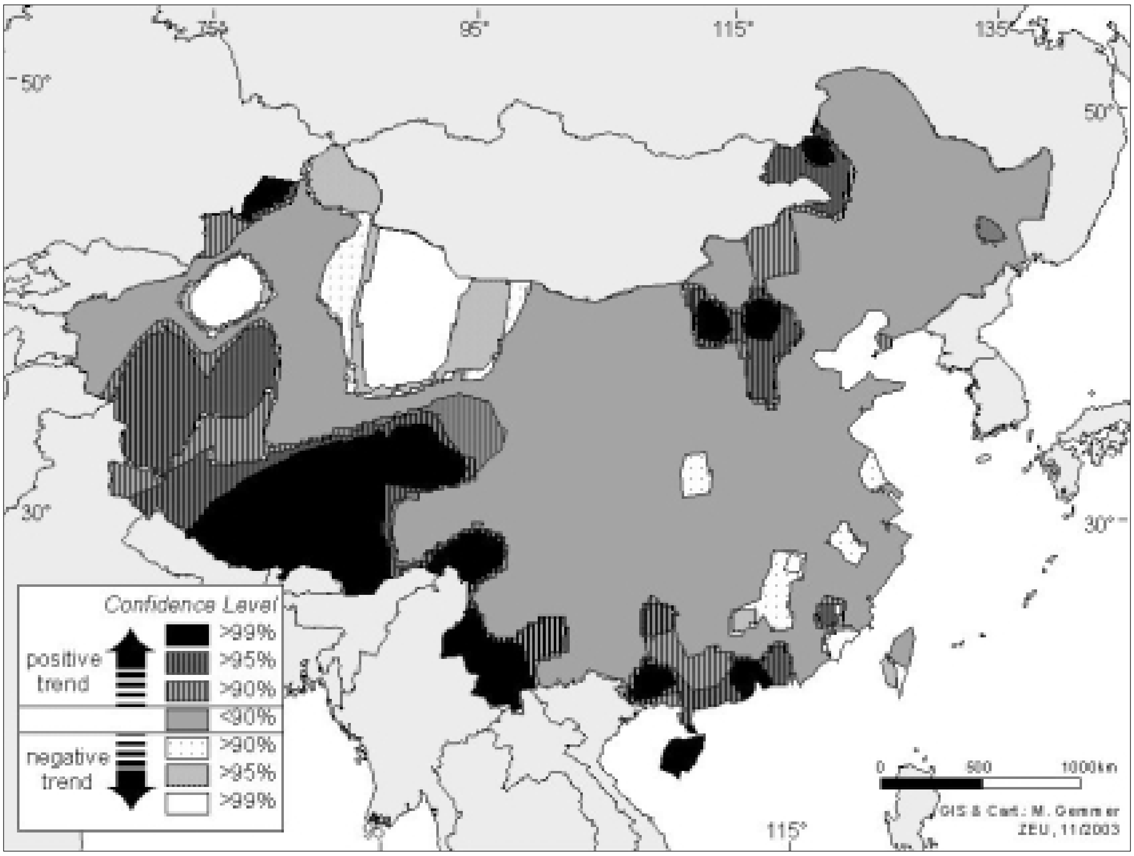

Figure 27: Mann-Kendall Temperature Trend Test September 1951-2002

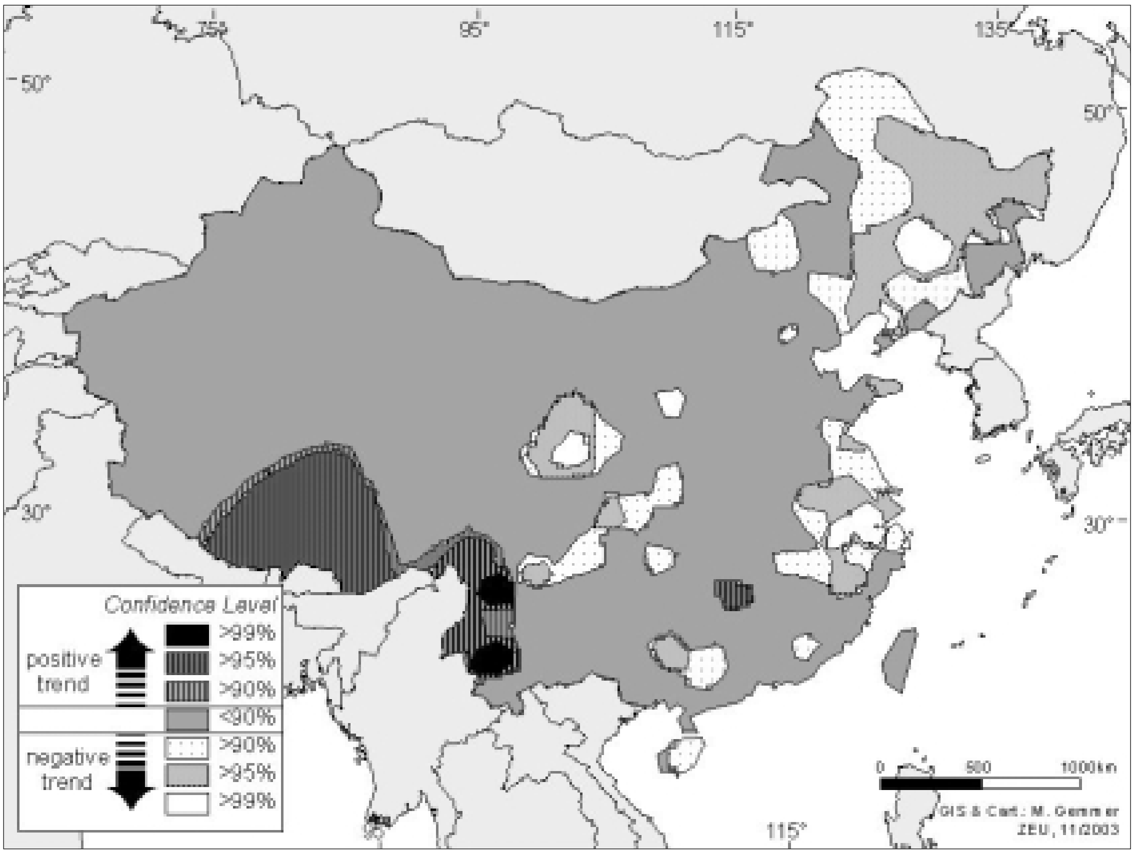

Figure 27 depicts concentrated belts and separated existences of positive and negative temperature trends in September. Positive trends can mainly be found in western Tibet and Xinjiang, the south-western and coastal region and in a distinct belt in the Huanghe and Huaihe river catchments (see **figure 16**). This belt follows the flow direction of the Huanghe between the topographical steps of the lowlands and the low mountain ranges. Negative trends are spread all over central and southern China. They are also concentrated in the arid region of Xinjiang, Qinghai and Gansu with the same spatial extent as in the four preceding months.

Temperature trends in October (**figure 28**) are characterised by a very low number of negative trends and a high number of positive trends at all confidence levels. Negative trends can be assigned to small areas in the northern Yangtze catchment and central Xinjiang province. Positive trends form a distinct belt through the eastern lowlands on the other hand. They cover an uninterrupted strip of China from Inner Mongolia right to Hainan island. Some isolated patterns of positive trends can also be recognised in central and south-west and western Tibet/Xinjiang.

Figure 28: Mann-Kendall Temperature Trend Test October 1951-2002

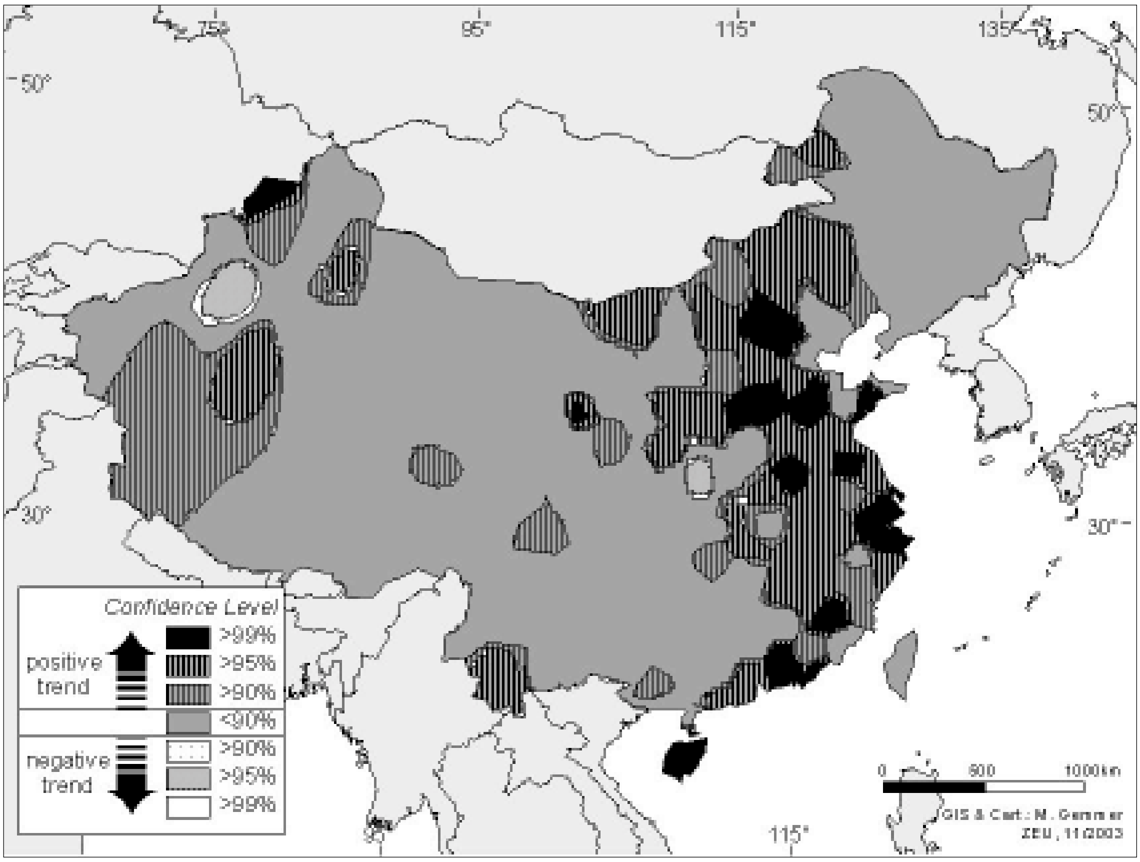

Only a small number of stations display negative temperature trends in November (**figure 29**). The balance of the trends and the distribution of positive trends is slightly similar to the October results but positive trends in November concentrate in western China again. They cover large parts of Tibet and Xinjiang, the western and eastern part of Inner Mongolia and are also spread in southern China without any recognisable underlying spatial agglomeration. The south-western Yunnan mountainous region experiences positive trends again for the 11th month now.

Figure 29: Mann-Kendall Temperature Trend Test November 1951-2002

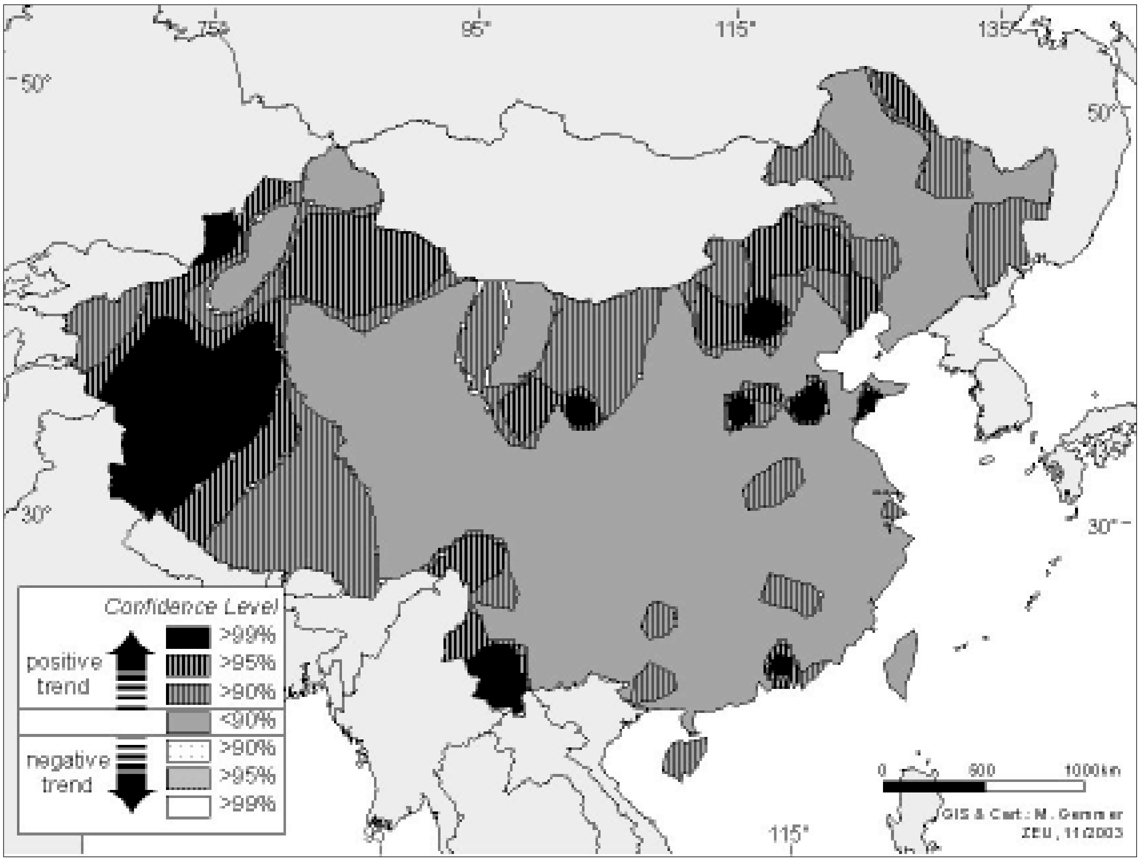

The map of temperature trends in December (**figure 30**) completes the visualisation of climate trends. A comparatively high number of positive and a small number of negative trends correspond to the trends which have been detected for previous months. A distinct warming trend covers the entire Chinese mainland except of central and south-east coastal China. The entire northern part of China is exposed to positive trends at high confidence levels. This is also valid for the mountainous region of the Qinghai-Tibet-Plateau and the catchment of the middle reaches of the Yangtze river along the topographical features. Negative trends can only be detected in central Yunnan and south-eastern Sichuan.

Figure 30: Mann-Kendall Temperature Trend Test December 1951-2002

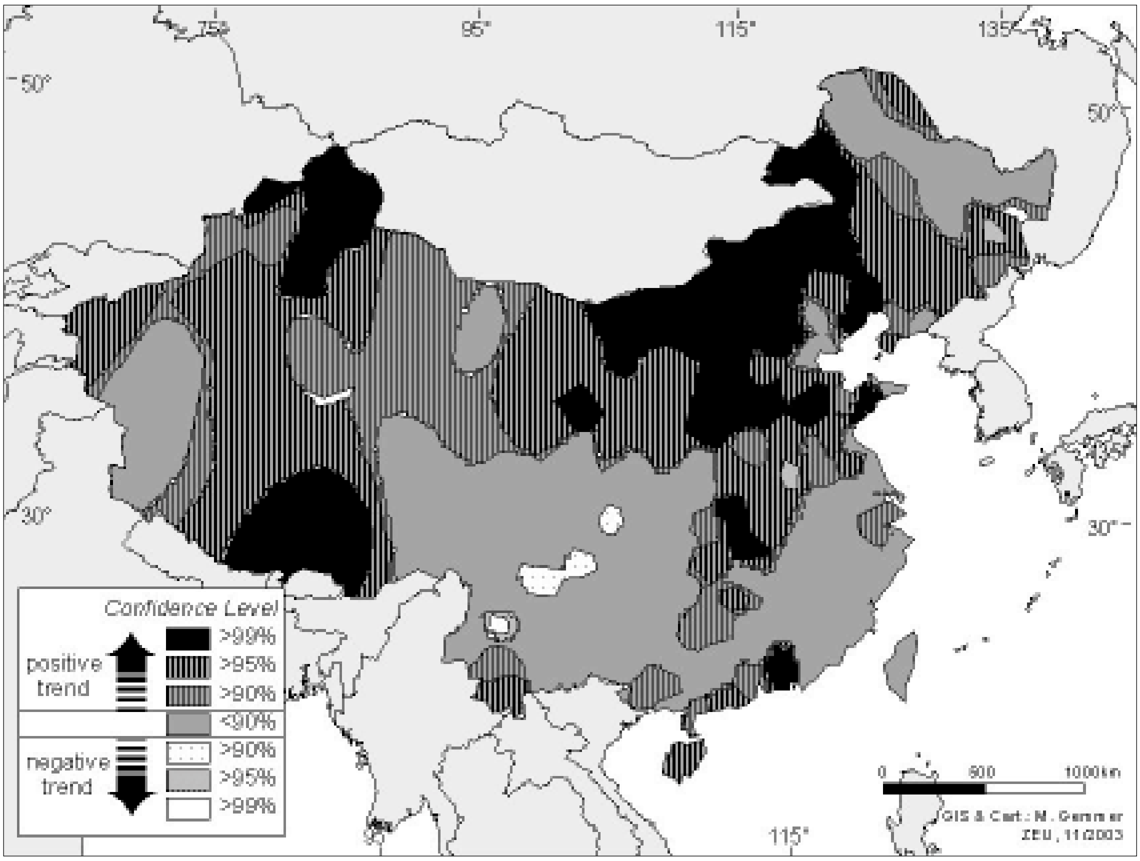

5 SUMMARY

Monthly precipitation and temperature trends of 160 stations in China from 1951-2002 have been analysed and interpolated. The Mann-Kendall trend test was applied to examine the monthly precipitation data. Significant positive and negative trends at the 90, 95 and 99% confidence levels were detected for numerous stations. The number, distribution and direction of the trends varied from month to month.

The detected trends were spatially interpolated by applying the Inverse Distance Weighted (IDW) interpolation method. The spatial illustration of the detected precipitation and temperature trends enables a better understanding of climatic changes or variations in China within the last 50 years. This counts especially for the spatial structure of the trends.

An agglomeration of precipitation trends can be observed in certain months including distinct trend belts especially in east and north-east China. Nevertheless, positive as well as negative trends can be noted simultaneously in each month. Negative precipitation trends are often followed by positive trends for the same area during the next month.

In the meantime positive temperature trends can be detected in north, north-east and west China. They can be visualised for large regions in every month and explain a warming trend of northern and western China. Negative temperature trends can only be found from October-December with a relatively limited spatial distribution.

The spatial interpolation of precipitation and temperature trend analysis results appears to be an adequate measure to give an understanding of the regional character of trends in China.

6 CONCLUSIONS/DISCUSSION AND OUTLOOK

GONG & WANG (2000) and QIAN & ZHU (2001) indicated significant negative precipitation trends for different regions in eastern China from 1954-1976 and subsequently positive trends from 1977-1998. QIAN & ZHU (2001) also describe distinct warm periods in northern China starting in the 1970s and in south China starting 10 years later. Four regions and eight regions respectively were created by merging different stations and analysing seasonal trends. However, monthly precipitation and temperature trends which were analysed in the present study show distinctive regional variations, also in eastern China, over the whole time period. They should not be neglected by merging and but be assessed monthly and locally. Artificially combining and averaging these data might also result in inhomogeneity of the time-series.

Therefore, spatial interpolation of precipitation and temperature trend analyses results appears to be an adequate measure to display the regional character of trends. The appearance of large area precipitation trends particularly in areas with a low station density in west and north-west China should not be misinterpreted. At present, long term precipitation data until 2002 with a higher spatial density in this area are not available. Temperature trends in north and north-east China on the other hand appear to be more reliable due to the high density of stations.

A first glance at the precipitation trends in China gives an indication towards negative trends in spring and autumn in east China which is accompanied by positive trends in summer. Temperature trends indicate a large scale climate warming especially during winter time. Positive temperature trends predominate and underline earlier findings which describe a decrease of absolute minimum temperatures and an increase of hot days (above 85% quantiles). The influence of atmospheric circulation on the regional to large-scale temperature anomalies was emphasised (HURRELL 1995, 1996). The Siberian High is a measure for the intensity of the winter monsoon over eastern Asia and accounts for more than 40% of the variance of the winter temperature over most part of China (GONG & WANG 1999). But the warming in eastern Asia took place not only in winter, but also in other seasons, such as summer and fall. The role of the east Asia monsoon, including the summer monsoon, still remains to be defined with regard to the observed warming. Nevertheless, an examination of interrelations of monthly precipitation and temperature trends between certain stations and regions will contribute towards the understanding of the spatial and temporal interrelation of climatic trends and variations.

The detected positive precipitation and temperature trends in the Yangtze river catchment give reason for concern with regard to climate induced risks. It is beyond controversy that human factors such as soil erosion, regulations of the river courses and wetland reclamation as well as changes in the precipitation regimes are important for aggregating floods at the Yangtze river (KING et al. 2001). Furthermore, negative precipitation trends especially in the north and northeast of China appear to be relevant with regard to agriculture and water supply of big cities such as Beijing (VARIS &

VAKKILAINEN 2001). These findings are underlined by positive temperature trends in north-east China, especially since precipitation, temperature and the associated environmental conditions of drought and wetness are the most direct factors affecting the hydrological cycle and the agriculture. They have a negative impact on the desertification and the food security in the northern region of China.

However, the results do not give any evidence regarding the future persistence of the observed trends. The question whether we are facing long-term climatic trends or the observed trends are only a part of long-term climatic variability remains yet unanswered. The secular changes of surface temperature and precipitation trends and their contribution to global warming are unknown completely.

7 REFERENCES

BECKER, S.; GEMMER, M. & JIANG, T. (2003a): 20th Century Precipitation Trends in the Yangtze River Catchment. Zentrum für internationale Entwicklungs- und Umweltforschung (ed.): *Discussion Papers* 14. ZEU, Giessen.

BECKER, S.; GEMMER, M. & JIANG, T. (2003b): Precipitation Trends in the Yangtze River Catchment. In: WORLD METEOROLOGICAL ORGANIZATION (ed.): Proceedings of the International Symposium on Climate Change (ISCC): 194-198. WMO/TD-NO. 1172. China Meteorological Press, Beijing.

BILL, R. (1999): Grundlagen der Geo-Informationssysteme. Vol. 2: Analysen, Anwendungen und neue Entwicklungen. Wichmann, Heidelberg (in German).

BUISHAND, T.A. (1982): Some Methods for Testing the Homogeneity of Rainfall Records. *Journal of Hydrology* 58: 11-27.

DE BY, R.A. (2001): Principles of Geographic Information Systems. ITC Educational Textbook Series 1. ITC, Enschede.

DOMRÖS, M. & PENG, G. (1988): The Climate of China. Springer, Berlin, Heidelberg.

DOMRÖS, M. (2001): Räumliche und zeitliche Variabilität der Sommerniederschläge in China. *Geographische Rundschau* 53 (10): 36-41 (in German).

GEMMER, M.; BECKER, S. & JIANG, T. (2003): Observed monthly precipitation trends in China 1951-2002. *Theoretical and Applied Climatology*. Accepted for publication/in print.

GEMMER, M. & KING, L. (2003): Human and Climatic Change Impacts on Yangtze River Floods. In: WORLD METEOROLOGICAL ORGANIZATION (ed.): Proceedings of the International Symposium on Climate Change (ISCC): 58-61. WMO/TD-NO. 1172. China Meteorological Press, Beijing.

GONG, D.Y. & WANG, S.W. (1999): Variability of the Siberian High and the Possible Connection to Global Warming. *Acta Geographica Sinica* 54: 125-133 (in Chinese).

GONG, D.Y. & WANG, S.W. (2000): Severe summer rainfall in China associated with enhanced global warming. *Climatic Research* 16: 51-59.

HURRELL, J. W. (1995): Decadal trends in the North Atlantic Oscillation: regional temperatures and precipitation. *Science* 269: 676-679.

HURRELL, J. W. (1996): Influence of variations in extratropical wintertime teleconnections on northern hemisphere temperature. *Geophysical Research Letters* 23: 655-668.

IPCC (Intergovernmental Panel on Climate Change) (2001): Climate Change 2001: The Scientific Basis. Cambridge University Press, Cambridge.

KING, L.; GEMMER, M. & WANG, R. (2001): Hochwasserschutz und Landnutzung am Yangtze. *Geographische Rundschau* 53 (10): 28-34 (in German).

MANIAK, U. (1997): Hydrologie und Wasserwirtschaft. Springer, Berlin.

QIAN, W. & ZHU, Y. (2001): Climate Change in China from 1880 to 1998 and its Impact on the Environmental Condition. *Climatic Change* 50: 419-444.

QIAN, W.; KANG, H.-S. & LEE, D.-K. (2002): Distribution of Seasonal Rainfall in the East Asian Monsoon Region. *Theoretical and Applied Climatology* 71: 151-168.

SCHÄFER, D. (2001): Rezente Klimaänderungen in China? *Geographische Rundschau* 53 (10): 42-46 (in German).

SMIT, B. & CAI, Y. (1996): Climate Change and Agriculture in China. *Global Environmental Change* 6 (3): 205-214.

VARIS, O. & VAKKILAINEN, P. (2001): China's 8 challenges to water resources management in the first quarter of the 21st Century. *Geomorphology* 41: 93-104.

YIN, Z.Y. (1999): Winter temperature anomalies of the north China plain and macroscale extratropical circulation patterns. *International Journal of Climatology* 19: 291–308.

ZHAI, P.M.; REN, F.M. & ZHANG, Q. (1999a): Detection of trends in China's precipitation extremes. *Acta Meteorologica Sinica* 57: 208-216.

ZHAI, P.M.; SUN, A.; REN, F.; LIU X.; GAO, B. & ZHANG, Q. (1999b): Changes of climate extremes in China. *Climatic Chang*e 42: 203-218.